공학박사학위논문

# Synthesis and Characterization of 30Kc19-based Protein Nanoparticles for the Application to Drug Delivery

약물 전달에 응용하기 위한 30Kc19를 이용한 단백질 나노입자의 제조 및 특성 연구

2015년 2월

서울대학교 대학원
공과대학 화학생물공학부
이 홍 재

# ABSTRACT

## Synthesis and characterization of 30Kc19-based protein nanoparticles for the application to drug delivery

Hong Jai Lee
School of Chemical and Biological Engineering
The Graduate School
Seoul National University

30Kc19 protein is a member of the 30K protein family from silkworm, having molecular weights of around 30 kDa. 30Kc19 protein is the most abundant among 30K proteins in the hemolymph. In previous studies, 30K proteins exhibited anti-apoptotic effect in various cells by gene expression or addition of 30K proteins in recombinant form produced from *Escherichia coli*. 30Kc19 also enhanced productivity and glycosylation by expression of a 30Kc19 gene or supplementation with a recombinant 30Kc19 protein. Additionally, 30Kc19 exhibited enzyme-stabilizing and cell-penetrating abilities *in vitro*.

In this study, it was hypothesized that supplemented 30Kc19 penetrated into the cell and enhanced the stability of the cellular enzyme, and investigated this

using *in vitro* and cellular assessments. The activity of isolated mitochondrial complex I / III was enhanced with 30Kc19 in dose-dependent manner while initial reaction rate was unchanged, suggesting that 30Kc19 enhanced enzyme stability rather than specific activity. For intracellular enzyme activity assessment, mitochondrial complex II activity in HeLa cells increased more than 50% with 30Kc19. The enhanced mitochondrial complex activity increased mitochondrial membrane potential and ATP production in HeLa cells with 30Kc19, by over 50%.

Then cell penetrating and enzyme stabilizing effect of 30Kc19 was exploited to efficient drug delivery. 30Kc19 and HSA were used as building block of protein nanoparticles to exploit both beneficial effect of 30Kc19 protein stability of HSA nanoparticles. 30Kc19-HSA nanoparticles were successfully prepared using the desolvation method, with uniform spherical morphology and stable dispersion. 30Kc19-HSA nanoparticles showed negligible toxicity when treated to cells, and 30Kc19-HSA nanoparticles also exhibited increase in cellular uptake compared with HSA nanoparticles.

Because stable 30Kc19-HSA nanoparticles were successfully synthesized and characterized, nanoparticles loaded with model enzyme cargo to investigated effect of 30Kc19 on cargo enzyme. 30Kc19-HSA nanoparticles loaded with β-galactosidase were uniformly spherical in shape, dispersed evenly in phosphate buffered saline and cell culture media, and released β-galactosidase in a sustained manner. The 30Kc19-HSA nanoparticles had negligible toxicity to animal cells and exhibited enhanced cellular uptake and intracellular stability of β-galactosidase in HeLa and HEK293 cells when compared with those of HSA nanoparticles. These results suggest that 30Kc19-HSA protein nanoparticles

could be used as a versatile tool for drug delivery to various cells.

Next, 30kc19-HSA nanoparticles were used to deliver actual therapeutic protein to cells. Fabry disease is a genetic lysosomal storage disease caused by deficiency of α-galactosidase, the enzyme that degrades neutral glycosphingolipids transported to lysosomes. Enzyme replacement therapy (ERT) using recombinant α-galactosidase is the only treatment available for Fabry disease. Because enhancing cellular delivery and enzyme stability is a challenge of ERT using α-galactosidase to maximize treatment efficacy, 30Kc19-HSA protein nanoparticles were used to enhance delivery and intracellular α-galactosidase stability. The 30Kc19-HSA nanoparticles had a uniform spherical shape and were well-dispersed. The 30Kc19-HSA nanoparticles had negligible toxicity to human cells. The nanoparticles exhibited enhanced cellular uptake and intracellular stability of the delivered α-galactosidase in human foreskin fibroblasts. Additionally, the nanoparticles enhanced globotriaosylceramide degradation in fibroblasts from a patient with Fabry disease. It is expected that 30Kc19-HSA protein nanoparticles will be used as an effective tool for efficient delivery and enhanced stability of drugs.

**Keywords**: 30Kc19 protein, mitochondrial complex, enzyme stability, protein nanoparticle, drug delivery, Fabry disease

**Student number**: 2006-21377

# Contents

## List of Figures

# Chapter 1.

# Research background and objectives

# Chapter 1. Research background and objectives

30Kc19 protein (30Kc19) is a major protein of the 30K protein family in silkworm hemolymph. Because anti-apoptotic effects of silkworm hemolymph were observed [1, 2], the potentially beneficial effects of silkworm hemolymph and the 30K proteins were studied [3-5]. In previous study, productivity of EPO was enhanced simultaneously by the expression of 30Kc19 [6, 7]. Although ATP generation was increased by the expression of 30Kc19, it has remained unclear as to how 30Kc19 enhances ATP generation, and thus mitochondrial function. Recently, it was reported that enzyme-stabilizing properties of 30Kc19 [8]. Because activity of enzyme decreases as the enzyme is denatured and becomes chemically changed by surrounding environment [9], stability of enzyme is strongly related with mitochondrial function Thus, It can be hypothesized that increased mitochondrial function with 30Kc19 are due to stabilized enzymes involved in mitochondrial function by 30Kc19.

The drug including chemicals, therapeutic enzymes, antibodies, and transcription factors has various targets, including receptors, enzymes in cytosols or inside microsomes [10], and DNA [11]. Among diverse techniques to deliver drugs to target, nanoparticles attract attention of researchers in drug delivery field for beneficial features of nano-sized particles. Protein-based nanoparticles have advantages such as higher storage and *in vivo* stability, non-toxicity to cells and tissues, and milder preparation condition that favorable to loaded therapeutics [12-14]. Albumin is appropriate protein for protein nanoparticles because it is biodegradable, nontoxic, and non-immunogenic. Albumin nanoparticles are synthesized in milder condition compared with

inorganic particles, and mass production of albumin nanoparticles can be easily achieved since large quantity of albumin is commercially available. Albumin has its own endocytosis route mediated by an albumin receptor located at caveolae. However, some cells lack or have a limited number of caveolae; thus, additional ligands are desirable to efficiently deliver albumin nanoparticles loaded with therapeutic agents into target cells. Maintaining drug cargo activity is also challenging, as enzyme cargo can be deactivated during the nanoparticle preparation process or after intracellular delivery.

In this research, 30Kc19 protein was applied to cellular enzyme to investigate whether it has beneficial effects on cellular delivery and enzyme stabilization. Then, in order to apply these beneficial effects of 30Kc19 protein to cellular drug delivery, protein nanoparticles were synthesized using 30Kc19 and HSA. Then model protein cargo was loaded on the 30Kc19-HSA protein nanoparticles, and effect of 30Kc19-HSA nanoparticles on intracellular uptake and stability of cargo was investigated. Finally, 30Kc19-HSA nanoparticles were applied to therapeutic protein delivery, α-galactosidase.

In summary, the objectives of this study are:

1. Stabilization of cellular mitochondrial enzyme complex activity through supplementation of 30kc19 protein
2. Synthesis of protein nanoparticles using 30kc19 protein and human serum albumin
3. Protein nanoparticles for protein cargo delivery using 30kc19 protein and human serum albumin

4. Protein nanoparticles for therapeutic protein delivery using 30kc19 protein and human serum albumin

In this study, effect of 30Kc19 on intracellular enzyme was investigated, and with cell penetrating activity this beneficial effect of 30Kc19 was applied to protein drug delivery by construction of 30Kc19-HSA hybrid protein nanocarrier. It is expected that be used as a versatile tool for intracellular delivery of therapeutic proteins, anti-cancer drug, antibodies, and cosmetic proteins.

# Chapter 2.

# Literature review

# Chapter 2. Literature review

## 2.1 Nanoparticles for drug delivery

The drug including chemicals, therapeutic enzymes, antibodies, and transcription factors has various targets; receptors located on cell surface, enzymes in cytosols or inside microsomes [10], and DNA [11] or other factors inside nucleus. However, a number of drug have little or no ability to penetrate into cellular membrane for targets are located inside cells to reach its target inside cells. Among diverse techniques to deliver drugs to target, nanoparticles attract attention of researchers in drug delivery field for beneficial features of nano-sized particles. Nanoparticles synthesized by various inorganic and organic materials are actively applied to effective drug delivery.

### 2.1.1 Terminology of nanoparticles

In the definition of nanoparticles by IUPAC, the term “nanoparticles” denotes that “Particle of any shape with dimensions in the $1 \times 10^{-9}$ and $1 \times 10^{-7}$ m range” [15]. Normally, the Particles under 100 nm exhibit novel properties different from the bulk material because nano-sized material shows size-dependent properties due to change in proportion of surface atoms, while a bulk material have constant physical properties regardless of its size since proportion of surface atoms to whole atoms becomes negligible. However, because other novel properties such as turbidity and stable dispersion are appear in particles lager than 100 nm, occasionally particles smaller than 500nm are considered nanoparticles. In the case of tubes or fibers, they are considered nanoparticles if

the dimension of cross section is nano-sized [16].

### 2.1.2 Classification of nanoparticles

Nanoparticles can be synthesized from diverse materials. In general, Nanoparticles divided into two classes, inorganic and organic nanoparticles for base material of nanoparticles (Fig. 2.1.1). Inorganic nanoparticles have many beneficial characteristics for drug delivery, including durability of core materials, abundant functional groups, and low cost of base materials. Inorganic nanoparticles also has unique functions such as fluorescent, magnetic properties, and photothermal abilities [17].

Magnetic nanoparticles, mainly superparamagnetic iron oxide nanoparticles, have been widely used as MRI contrast agent [18-20]. Mass production of magnetic nanoparticles is well developed and particle size can be controlled at ease. Using external magnetic field, magnetic nanoparticles can be also moved and fixed to desired location [21]. This magnetic-responsive feature is particularly helpful in *in vivo* application because homing and fixing drug on desirable place against blood flow is one of the challenging issues [22]. Mesoporous silica nanoparticles (MSNs) are actively applied in drug delivery due to their high surface area for drug loading [23]. The MSNs also have biocompatibility so recently FDA approved MSNs for cancer targeted probe [24]. Furthermore, The MSNs can be easily modified functional ligands to therapeutic targets [25]. Gold nanoparticles has been widely used in nanotechnology since they have unique optical and electric properties, low toxicity and controlled size, suitable for application drug delivery. Gold

nanoparticles used for drug delivery are frequently combined with other nanomaterials such as polymers, magnetic nanoparticles, and carbon nanotubes [26-29]. Quantum dots (QDs) are synthesized from semiconductors and have fame for its photo-physical properties. Fluorescence of QDs have high brightness and low photobleaching, contrary to other chemical and biological fluorescent. For drug delivery, Similar to gold nanoparticles, QDs are combined with other drug delivery materials as imaging agent rather than used for drug delivery [30-32].

Recently, organic nanoparticles attract increasing interest of drug delivery researchers. Because organic nanoparticles are bio-degradable and shows low toxicity. Micelles, liposomes, polymeric nanogels, dendritic polymers, and polymeric nanoparticles are synthesized and investigated for biomedical application. Micelles are synthesized using supramolecular amphiphilic copolymers consisting of amphiphilic blocks. Micelles are formed as the hydrophobic blocks aggregate to inside while hydrophilic blocks locate to outside of micelles [33-36]. Diverse micelles can be synthesized by adjusting block length and number. Poly (ethylene glycol) (PEG) is popular hydrophilic block of micelles since PEG has biocompatibility; PEG does not interact with *in vivo* proteins or antibody [37-39]. The polymers consisting micelles can be modified with targeting ligand, or pH-responsive polymers for effective drug delivery [40, 41].

Similar to micelles, polymer liposomes are synthesized using amphiphilic block copolymers. However, contrary to micelles, liposome are formed as bilayer of spherical structure [42, 43]. Polymer liposomes internalize to cells via adhesion with bilayer of the cell membrane, and fusing with cell membrane.

Polymeric liposomes are biodegradable and some liposome formulations for drug delivery have been approved by FDA for clinical use [44].

Polymer nanogels has sophisticated highly porous structure, synthesized with crosslinked polymer chains via self-assembly [45]. With this porous structure, polymer nanogels can contain large volume of drugs and release drugs in controlled manner [46]. Polymeric nanogels are flexible and can swell in specific environment, i.e., pH, temperature, and ionic strength, can be applied to stimuli-response drug delivery [47]. Furthermore, surface of nanogels can be properly modified with functional groups to achieve targeted delivery and low cellular toxicity [48].

Dendritic polymers are usually synthesized with polyamidoamine (PAMAM), poly (propyleneimine), polyaryl ethers and polylysine [49]. Formation of dendritic polymers start with monomeric units, and in several steps new branches are added to polymers. In the controlled environment, branching occurs uniformly throughout each branching step and tree-like structure is developed. Dendritic polymers have void space between branches that can retain high volume of drug [50]. Dendritic nanoparticles has beneficial functions for efficient drug delivery such as low polydispersity, low viscosity, and bio compatibility [49, 51].

Polymeric nanoparticles is synthesized from amphiphilic co-polymers such as poly (lactic- co-glycolic acid) (PLGA) and polyanhydrides. Because PLGA and polyanhydrides has biodegradable, polymeric nanoparticles have great advantage in cellular drug delivery [52, 53]. Proteins, the natural hydrophilic polymers also efficient materials for synthesize polymeric nanoparticles because of drug-loading capacity, biocompatibility and less clearance by

reticuloendothelial system (RES) [54]. Proteins including gelatin, collagen, casein, albumin and whey protein was used source material of protein nanoparticles [55, 56].

## 2.2 Albumin nanoparticles

Among various nanocarrier systems for drug delivery, protein-based nanoparticles have advantages such as higher storage and *in vivo* stability, non-toxicity to cells and tissues, and milder preparation condition that favorable to loaded therapeutics [12-14]. Albumin is a protein for protein nanoparticles, because it is biodegradable, nontoxic, non-immunogenic, and high solubility in water. The drug can be loaded to albumin nanoparticle matrix because albumin has abundant drug binding sites [57, 58]. Furthermore, albumin can adsorb electrostatically both positively and negatively charged therapeutic molecules because of high content of charged amino acids (e.g. lysine) [59, 60]. Albumin nanoparticles are synthesized in milder condition compared with inorganic particles, and mass production of albumin nanoparticles can be easily achieved since large quantity of albumin is commercially available.

### 2.2.1 Albumins for nanoparticle production

Various type of albumins are commercially available. Albumins from egg white (ovalbumin), bovine serum (bovine serum albumin, BSA), and human serum (human serum albumin, HSA) are major, whereas albumins from soybeans, milk, and grains are also available. Ovalbumin is widely used protein

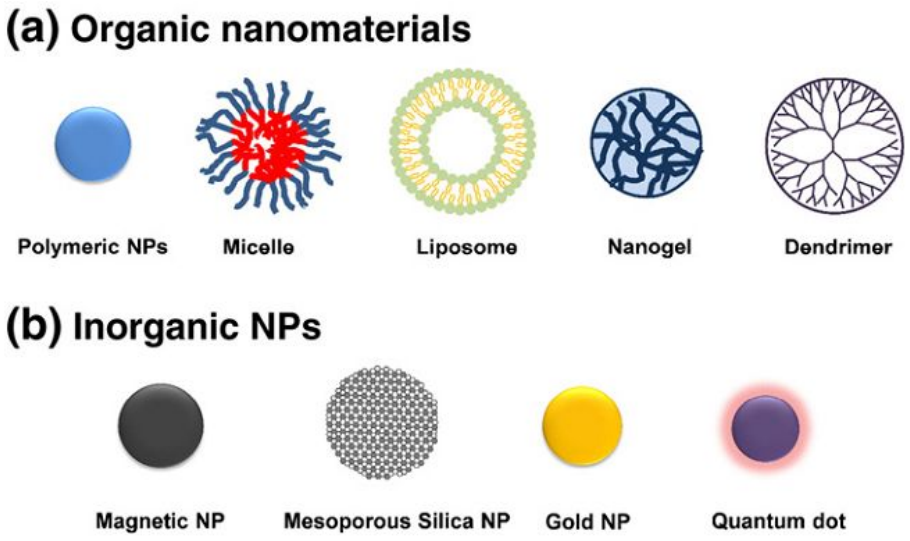


**Figure 2.1.1** Representative structures of various multifunctional NPs for drug delivery [61]. (a) Organic nanomaterials and (b) inorganic nanomaterials.

in food industry. It has 385 amino acid residues and one internal disulfide bond. Its molecular weight is 47,000 Da and it has isoelectric point (pI) of 4.8. OVA has low cost compared with other proteins and exhibits pH and temperature-sensitive properties, having advantage for controlled drug release [62]. BSA has a molecular weight of 69,323 Da and a pI of 4.7. BSA is widely used for drug delivery in in the pharmaceutical industry for its abundance, low cost, ligand-binding properties [63, 64]. HSA has advantage over BSA because it can avoid a possible immunogenicity *in vivo*. HSA is the most abundant plasma protein (35–50 g/L human serum), with 66,500 Da molecular weight and contains 35 cysteinyl residues forming one sulfhydryl group and 17 disulfide bridges. HSA is extremely stable protein against pH (4–9), temperature (60 °C for up to 10 h) and organic solvents [65]. From these features, HSA are widely used as building block of protein nanoparticles for drug delivery to cells and *in vivo* application [66, 67].

### 2.2.2 Preparation of albumin nanoparticles

Albumin nanoparticles can be prepared by desolvation, emulsification, thermal gelation, and nano spray drying. In desolvation process, the desolvation process exploits controlled aggregation of albumin with decreasing hydration by desolvation agent, mainly ethanol. Ethanol is added to aqueous albumin solution under continuous stirring [59, 68]. As addition of ethanol, albumin is no longer stably dissolved since water molecules are detached from albumin molecules due to ethanol. With appropriate pH and ionic strength, uniformly-sized albumin aggregates are formed. However, these aggregates are not

sufficiently stabilized and consequently redissolved again when being dispersed with water. Therefore, after albumin aggregates further stabilized by crosslinking with crosslinking agent, mainly glutaraldehyde [65, 69]. Crosslinking takes place at amino moieties in lysine residues and arginine moieties in guanidino side chains of albumin by a condensation reaction with the aldehyde-group of glutaraldehyde (Fig. 2.2.1A). Alternatively, methyl polyethylene glycol modified oxidized dextran (Dextranox-MPEG) was used for crosslinking of albumin nanoparticles creating a polyethylene oxide surface layer on surface of nanoparticles [70]. These dextranox-crosslinked nanoparticles exhibited highly minus-charged surface, ensures stable dispersion in solution. Crosslinked nanoparticles are collected by centrifugation and washed with buffers to eliminate the free albumin and the excess crosslinking agent.

Emulsification is routinely used technique for preparation of polymeric nanoparticles. Emulsification can be achieved by thermal or chemical treatment [71]. In thermal emulsification process, albumin contained in the oil phase are homogenized to droplets at a high speed, then heated at 175 to 180 °C for 10 min to stabilization [72]. This mixture containing albumin is cooled and gathered by centrifugation. Alternatively, Emulsified albumin droplet is denatured by crosslinking agent 2,3-butadiene or formaldehyde [73].

In thermal gelation albumin is unfolded by heat and then protein–protein interactions including hydrogen bonding, electrostatic, hydrophobic interactions and disulfide–sulfydryl interchange reaction [74-76]. With appropriate protein concentration, pH, and ion strength, various nanoparticle size was obtained. In the case of BSA, stability was maximum at pH 5 and Glucose had a great

stabilizing effect on the thermal denaturation of BSA. Denaturation of BSA caused loss of α-helical structure and the formation of ordered non-native β-sheet structure associated with aggregation [77].

Spray drying is traditional method for produce powder from liquid in pharmaceutical industry. In the new spray drying for produce nano-sized particles, Nano Spray Dryer, the piezoelectric-crystal-driven ultrasonic frequency vibrates the mesh, injecting millions of precisely sized droplets from the holes and generating the aerosols. And then electrostatic precipitator collects of fine particles with high efficiency with the electrostatic particle collector, by using electrostatic field that accelerates the deposition of negatively charged particles onto the inner wall of particle collecting electrode [78]. Fig. 2.2.1A illustrates the functional principle of an electrostatic particle collector in the Nano Spray Dryer. BSA nanoparticles were formed in a single step using this Nano Spray Dryer, with spherical nanoparticles in 460 nm at high yield.

### 2.2.3 Surface modification of albumin nanoparticles

Due to functional groups on surface of albumin nanoparticles, various surface modifications are possible. Ligands for modification are usually attached to the nanoparticle surface via covalent bonding or electrostatic adsorption. Surface modification is performed to achieve stability enhancement of the nanoparticle, *in vivo* circulation half-life, or targeting to desirable drug target.

Surfactant coating is used to reduce toxicity of anticancer chemicals, such as doxorubicin. When coated with polysorbate 80, HSA nanoparticles loaded with

doxorubicin exhibited reduced hematological, cardiac and testicular toxicities [79-81].

In desolvation method, nanoparticles are stabilized using glutaraldehyde as crosslinking agent. However, residual glutaraldehyde can be cytotoxic and undesirable reaction with drug result in hamper activity of drug [82]. To avoid undesirable effect of crosslinker, BSA nanoparticles coated with cationic polymers, polyethylenimine (PEI) rather than glutaraldehyde in Bone morphogenetic protein-2 (BMP-2) delivery [83, 84]. Additionally, the surface charge of the PEI-coated BSA nanoparticles shifted to positive, contrary to nanoparticles without PEI coating.

The thermo-responsive poly (N-isopropylacrylamide-coacrylamide)-block-polyallylamine (PNIPAM-AAm-b-PAA) was used to deliver the anti-cancer drug, adriamycin. PNIPAM-AAm-b-PAA coated nanoparticles showed slower release of adriamycin, whereas faster release was observed with higher temperature than critical point. These results suggest possibility to tumor targeted treatment using local heat to tumor location [85, 86].

Polyethylene glycol (PEG) is widely applied to proteins and particles for increase circulation half-life, decrease immunogenicity, and promote their accumulation in tumors due to enhanced permeability and retention (EPR) effect. However, PEGylated BSA nanoparticles showed slower drug release compared to non-PEGylated counterparts due to PEG acted as diffusion barrier against loaded drug [87, 88].

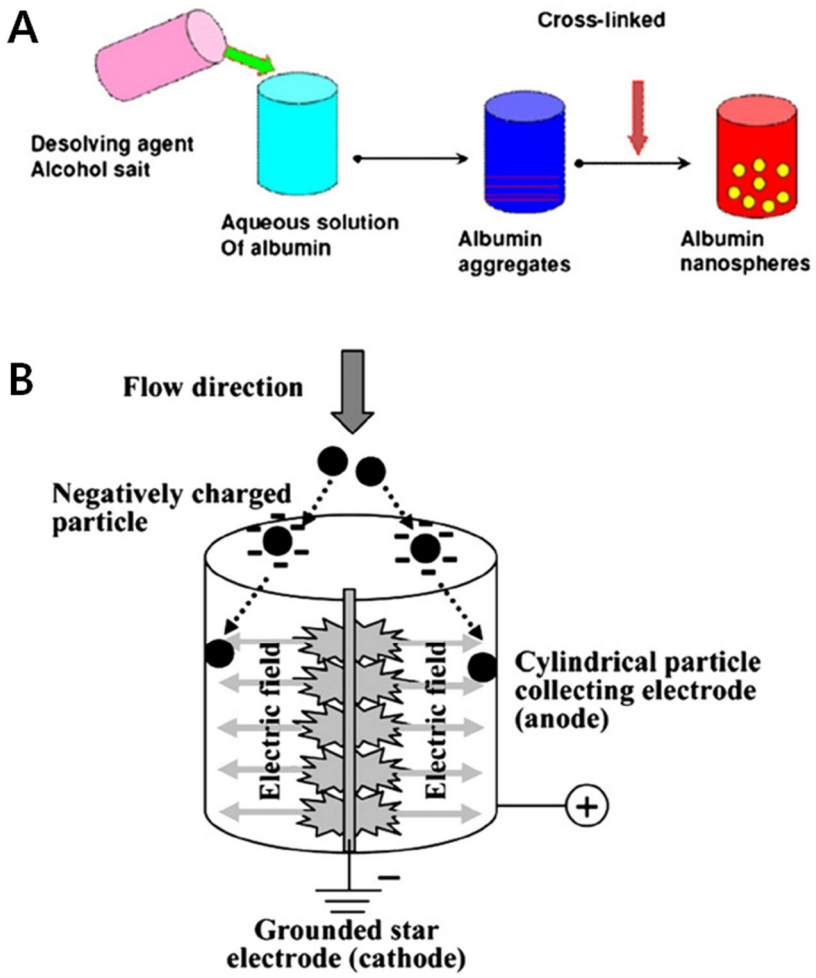


**Figure 2.2.1** Preparation of albumin nanoparticles by (A) desolvation (simple coacervation) method [89] and (B) nano spray drying [78].

Folic acid (FA) is a low molecular weight (441 Da) vitamin. FA actively used in cancer targeting ligand since FA receptor is overexpressed in human cancer cells, particularly in ovarian carcinomas whereas exhibit restrict expression in normal cells [90, 91]. FA has great advantage in drug targeting for cancer because it is stable and less expensive compared with protein ligand or antibody, FA is also non-immunogenic as it is small chemical compound [92].

Various and peptides and proteins are used for surface modification of albumin nanoparticles. Cyclic arginine–glycine–aspartic acid (RGD) peptide is a ligand that bind to αvβ3 integrin, membrane receptor for extracellular matrix ligands such as vitronectin and fibronectin overexpressed in cancer cells [93, 94]. When bonded to nanoparticles, RGD peptide exhibited not only effective targeting to cancer cells but also stabilization of BSA nanoparticles sterically. To target the brain, apolipoprotein E (Apo E) was covalently bound to HSA nanoparticles to deliver drugs across the blood brain barrier. After intravenous injection into mice, only the ApoE-modified nanoparticles were detected in brain capillary endothelial cells and neurons, whereas no uptake was detectable with unmodified nanoparticles [95, 96].

Monoclonal antibodies (mAb) are one of most applied ligands for specific tumor targeting. The human epidermal growth factor receptor-2 (HER2), the famous for breast cancer marker, is targeted by the humanized anti-HER2 specific antibody trastuzumab (Herceptin®) [97]. HSA nanoparticles modified with trastuzumab successfully targeted and internalized to HER2-overexpressing BT474, MCF7 and SK-BR-3 cells. Many cancer cells exhibit an overexpression of the epidermal growth factor receptor (EGFR), so cetuximab, a humanized IgG1 mAb targeting EGFR was also used to surface modification

of HSA nanoparticles to enhance targeting to EGFR-expressing colon carcinoma cells [98].

### 2.2.4 Uptake of albumin nanoparticles

Albumin internalizes to cells via caveolae-mediated endocytosis. When albumin is close to cell surface, it binds to 60-kDa glycoprotein receptor, gp60, located on cell surface. Once albumin is bound to gp60, and then gp60 binds to caveolin-1, intracellular protein and invagination of the cell membrane is occurred to form endocytic vesicles (Fig. 2.2.2) [99, 100]. Albumin nanoparticles can also utilize cellular uptake route via gp60. Albumin loaded with anticancer drug paclitaxel exhibited increased anticancer activity due to increased cellular uptake via gp60. Additionally, albumin nanoparticles also exploit SPARC, an extracellular matrix glycoprotein that is overexpressed in various cancers when applied to anticancer drug delivery. In a preclinical study using radiolabeled paclitaxel, albumin nanoparticles loaded with anticancer drug showed enhanced localization in solid tumors, mediated by EPR effect, which is due to angiogenesis, hypervasculature, a defective vascular architecture and an impaired lymphatic drainage [99, 101, 102].

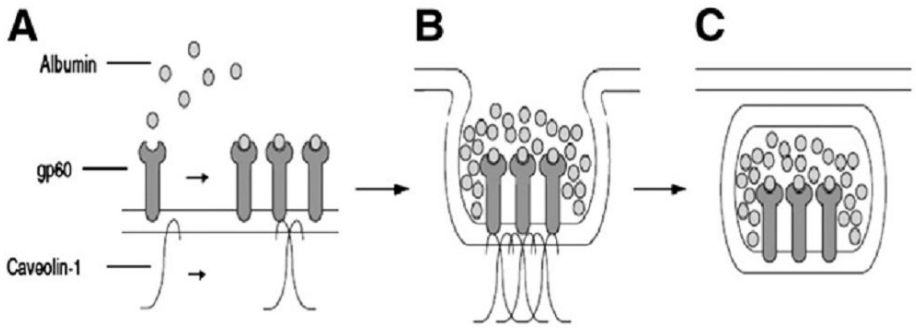


**Figure 2.2.2** Albumin receptor-mediated uptake of intravascular constituents and transcytosis across the vascular endothelium [100]. (A) Albumin receptor (gp60) binds albumin which in turn results in binding the induction of caveolin-1; (B) caveolin-1 induces membrane budding and internalization, trapping free and protein-bound plasma constituents; (C) formation of caveolae, leading to transcytosis and extravascular deposition of the caveolae contents.

# Chapter 3.

# Experimental procedures

# Chapter 3. Experimental procedures

## 3.1 Production of recombinant 30Kc19 protein

The 30Kc19 gene from 30Kc19 cDNA was obtained from the total RNA of *Bombyx mori*, amplified using the polymerase chain reaction, and inserted into the pET-23a expression vector (Novagen, Madison, WI, USA) with a T7 tag at the N-terminus and a 6 × His tag at the C-terminus. 30Kc19 was produced using *E. coli* BL21 (Novagen) and transformed with a constructed vector. Cells were cultured in LB medium containing 100 μg/ml ampicillin at 37°C and induced with 1 mM isopropyl-β-d-thiogalactopyranoside. The cells were further incubated for 4 h at 37°C, harvested, and then disrupted by ultrasonication. After centrifugation, the 30Kc19 protein was purified from the supernatant using a HisTrap HP column (GE Healthcare, Uppsala, Sweden) and dialyzed with phosphate buffered saline (PBS) using a desalting column (GE Healthcare). The purity of the 30Kc19 protein was > 90% (data not shown), and the purified 30Kc19 protein was stored at −70°C. The quantitative analysis of the 30Kc19 protein was performed using a Micro BCA kit (Thermo Fisher Scientific Inc., Rockford, IL, USA).30Kc19 protein was expressed from *E. coli* BL21 and purified using His-tag affinity chromatography. Final purity was assessed by SDS-PAGE.

## 3.2 Cell culture

HEK293T, HEK293, HeLa, human fibroblast cells were cultured in DMEM supplemented with 10% FBS and 1% penicillin/streptomycin (PS, Gibco).

## 3.3 Mitochondria isolation

Mitochondria were isolated from HEK293T cells using differential centrifugation [103]. HEK293T cells were cultured in a T25 culture flask. Confluent cells were washed, detached, and resuspended in mitochondria isolation buffer (1 mM EGTA, 250 mM sucrose, 5 mM HEPES) and then passed through a 22 1/2 gauge needle 10 times to break the plasma membranes. Following centrifugation (700 g, 10 min), mitochondria contained in supernatant were further separated by a second centrifugation step (7,000 g, 10 min), the pellet containing mitochondria was isolated from supernatant containing a mixture of microsomes, cytosol, and destroyed plasma membrane.

## 3.4 Western blotting

To investigate uptake of 30Kc19 to HeLa cells and mitochondria, HeLa cells were seeded and incubated overnight. Following 1 or 24h incubation with the 200 μg/ml of 30Kc19, cells were detached and subcellular fractionation was performed as described above to separate mitochondria (Mito) and microsomes + cytosol (Mi+Cy) fraction from homogenized cells. And then presence of 30Kc19 in mitochondria and cytosol was investigated by western blotting using 30Kc19 antibody.

## 3.5 Mitochondrial activity assay

For the *in vitro* mitochondrial complex I / III activity assessment, isolated mitochondria from HEK293T cells were added to 50 mM phosphate buffer

containing 100 µM NADH, 1.5 mM $NaN_3$, 50 µM oxidized cytochrome c (Sigma-Aldrich), and 30Kc19 followed by incubation at 37°C. The absorbance of the solution at 550 nm was recorded as a function of time [104]. The intracellular mitochondrial activity was assessed using the MTT (3-(4,5-dimethylthiazol-2-yl) 2,5-diphenyltetrazolium bromide) assay. HeLa cells were seeded in a 96-well plate at a density of 2,500 cells/well and incubated overnight. Culture medium were exchanged with fresh medium containing the 30Kc19 protein and further incubated. Following a 24h incubation, MTT solution (0.5 mg/ml) was added to each well and incubated for 2.5 h. After solubilization with buffer (20% SDS (w/v), 40 % dimethylformamide, pH 4.8), the absorbance at 560 nm was recorded using a microplate reader. Absorbance data were normalized with cell number, counted using a hemocytometer, to determine MTT reduction per cell.

## 3.6 Estimation of mitochondrial membrane potential and ATP generation

The mitochondrial membrane potential of HeLa cells was assessed using JC-1 (5,50,6,60-tetrachloro-1,10,3,30-tetraethylbenzimidazolylcarbocyanine chloride, Sigma-Aldrich) [105]. HeLa cells were seeded in 96-well plates and treated with 30Kc19 for 24 h. Cells were washed with PBS, and 100 µl of 2.5 µg/ml JC-1 solution in PBS was added to each well. Cells were incubated for 30 min at 37°C and washed twice with PBS. Emission fluorescence was measured using a spectrofluorometer (TEKAN, Grödig, Austria) with an excitation wavelength of 485 nm. The mitochondrial membrane potential is presented as

the ratio of emission fluorescence (590 / 535 nm). For the assay of ATP generation, HeLa cells were seeded in 96-well plates and treated with 30Kc19 for 24 h. Cells in each well were detached and suspended in 100 μl of fresh culture medium. The ATP content in the cell suspension was measured using an ATP bioluminescent somatic cell assay kit (Sigma Aldrich).

## 3.7 Preparation of nanoparticles

HSA-30Kc19 protein nanoparticles were prepared using the desolvation method. HSA (Sigma Aldrich, St. Louis, MO, USA), the 30Kc19 protein (30Kc19 wt.% of 0– 100%, total 1 mg), and 40 μg β-galactosidase (Sigma Aldrich) were dissolved in 500 μl Tris-HCl buffer (pH 9.0) under constant stirring (1000 rpm) at room temperature. Two ml of 100% ethanol was added drop wise using a syringe pump to form nano-sized protein aggregates for loading β-galactosidase. After desolvation, the 30Kc19-HSA nanoparticles loaded with β-galactosidase were crosslinked by adding 5 μl 10% glutaraldehyde aqueous solution and were stirred for 1 hour at room temperature. The nanoparticles were purified by centrifugation (Sigma Aldrich) at 12000 × g and 4°C for 20 min. The supernatant was discarded and the nanoparticle pellet was resuspended in PBS buffer. The prepared protein nanoparticles were centrifuged again and washed with PBS buffer three times.

## 3.8 Size and zeta potential of the nanoparticles

The particle size and zeta potential of the prepared nanoparticles were

determined with an electrophoretic light scattering (ELS) spectrophotometer (ELS-8000, Otsuka, Tokyo, Japan). The protein nanoparticles were centrifuged and resuspended in deionized water prior to the experiment. The size and zeta potential of the nanoparticles were determined using the corresponding mode of the ELS spectrometer according to the manufacturer's instruction.

## 3.9 Scanning electron microscopy (SEM) analysis of the nanoparticles

An SEM analysis was performed to visualize the morphological characteristics of the protein nanoparticles. A drop of nanoparticle aqueous solution was placed on a 12 mm circular coverslip, lyophilized using a freeze-dryer (Hanil, Seoul, Korea), and sputter-coated with Pt. SEM images were obtained using a field emission SEM (Carl Zeiss, Oberkochen, Germany). The acceleration voltage was 2.0 kV, and magnification was 50,000×.

## 3.10 β-galactosidase loading efficiency of the nanoparticles

β-Galactosidase was labeled with green fluorescent Alexa Fluor® 488 using a protein labeling kit (Invitrogen, Carlsbad, CA, USA) according to the manufacturer's instructions. The protein nanoparticles were synthesized as before to determine β-galactosidase loading efficiency, except that the β-galactosidase was labeled with Alexa Fluor® 488 rather than intact enzyme. The nanoparticle solution was centrifuged, and the supernatant was collected. The efficiency of β-galactosidase loading was determined indirectly by

measuring the initial fluorescence of the β-galactosidase added and that remaining in the supernatant. A standard curve of Alexa Fluor® 488 fluorescence intensity and β-galactosidase concentration was prepared prior to the experiment.

## 3.11 *In vitro* β-galactosidase release from nanoparticles

To assess *in vitro* β-galactosidase release from nanoparticles, 1 mg/ml of 30K-HSA nanoparticles loaded with labeled β-galactosidase in PBS were placed in a shaking incubator at 37°C and 200 rpm. The β-galactosidase released was separated from the nanoparticles by centrifugation at 12000 × g for 20 min. Then, the fluorescence of the labeled enzyme was measured and quantified using a standard curve.

β-Galactosidase activity of the enzyme released from the nanoparticles was determined using a β-gal assay kit (Invitrogen), according to the manufacturer's instructions. Briefly, 5 μl of sample was added to each well of a 96-well plate containing 50 μl of cleavage buffer (60 mM $Na_2HPO_4•7H_2O$, 40mM $NaH_2PO_4•H_2O$, 10 mM KCl, 1 mM $MgSO_4•7H_2O$, pH 7) and 17 μl of 4 mg/ml o-nitrophenol-β-D-galactoside (Sigma-Aldrich) aqueous solution and then incubated for 30 min at 37°C. A pale-yellow color developed during the incubation. After the incubation, 125 μl of stop buffer (1 M $Na_2CO_3$) was added to each well, and absorbance was read at 405 nm using an enzyme-linked immunosorbent assay (ELISA) reader (Thermo LabSystems, Milford, MA, USA).

## 3.12 Cell viability assay

To assess cytotoxicity of the 30K-HSA nanoparticles, HeLa and HEK293 cells were seeded on a 96-well plate at 70% confluency, and nanoparticles in DMEM (4 μg/ml β-galactosidase content in media) were added and incubated for 24 h at 37°C in a 5% CO2 incubator. Then 0.5 mg/ml MTT (3,(4,5-dimethylthiazol-2-yl)2,3-diphenyl-tetrazolium) was added to the media and incubated for 2 h. The formazan crystals that developed were solubilized with dimethyl sulfoxide (Sigma-Aldrich), and absorbance was measured at 560 nm using the ELISA reader.

## 3.13 Cellular uptake of nanoparticles

Cellular uptake of the protein nanoparticles was visualized by confocal microscopy. HeLa and HEK293 cells were seeded on an 8-well chamber plate and incubated overnight. Alexa Fluor® 488-labeled nanoparticles in DMEM (4 μg/ml β-galactosidase content in media) were added and incubated for 12 h at 37°C. After the incubation, the medium was exchanged with DMEM supplemented with 10% fetal bovine serum (FBS) and incubated for an additional 1 h. Nanoparticle-treated cells were washed with PBS twice, fixed in 4% paraformaldehyde for 20 min, and permeabilized with 0.25% Triton X-100 in PBS. Nuclei were stained with Hoechst 33342 for 10 min. A confocal laser microscope (CLM; EZ-C1, Nikon, Tokyo, Japan) was used to observe intracellular fluorescence and images were taken using the manufacturer's software (Nikon).

Cells in a 24-well plate were treated with Alexa Fluor® 488-labeled protein nanoparticles for 12 h as preparation for the flow cytometry analysis. The cells were washed with PBS twice, detached with 0.25% trypsin-EDTA, collected, and washed with PBS by sequential centrifugation. Alexa Fluor® 488-positive cells were identified using a FACSAria II (BD Bioscience, San Diego, CA, USA).

To assess α-Galactosidase cellular uptake of nanoparticles, human foreskin fibroblasts were seeded in a 96-well plate and incubated overnight. Alexa-Fluor® 488-labeled nanoparticles in DMEM (4 μg/ml α-galactosidase content in media) were added to the wells and incubated for 12 h at 37°C. After the incubation, the cells were washed with PBS, and cell fluorescence was determined with a fluorometer (Tecan, Vienna, Australia).

Cellular uptake of the protein nanoparticles loaded with α-galactosidase into cells was visualized by confocal microscopy. Human foreskin fibroblasts were seeded on an 8-well chamber plate and incubated overnight. Alexa-Fluor® 488-labeled nanoparticles in DMEM (4 μg/ml α-galactosidase content in media) were added to the wells and incubated for 12 h at 37°C. After the incubation, the media were exchanged with DMEM supplemented with 10% fetal bovine serum (FBS) or 10% FBS with Lysotracker (Sigma Aldrich) to target lysosomes and further incubated for 1 h. Nanoparticle-treated cells were washed with PBS twice, fixed in 4% paraformaldehyde for 20 min, and permeabilized with 0.25% Triton X-100 in PBS. Cell nuclei were stained with Hoechst 33342 for 10 min. A confocal laser microscope (EZ-C1, Nikon, Tokyo, Japan) was used to observe intracellular fluorescence, and images were taken using the manufacturer's software (Nikon).

## 3.14 Protein cargo activity of nanoparticle-treated cells

β-Galactosidase activity of cells treated with nanoparticles was determined using a β-gal assay and X-gal staining. HeLa and HEK293 cells were seeded on a 24-well plate at 70% confluency, and nanoparticles in DMEM (4 μg/ml β-galactosidase content in media) were added and incubated 24 h at 37°C in a 5% CO2 incubator. Medium was changed with fresh DMEM after the incubation with nanoparticles and incubated for an additional 72 h. Then, the medium was exchanged for DMEM supplemented with 10% FBS for 1 h. The cells were washed twice with PBS, and 100 μl of RIPA buffer was added to each well to obtain the cell lysate. After a 10 min incubation at room temperature, 10 μl of cell lysate was placed in wells of a 96-well plate, and the β-gal assay was performed as described previously.

HeLa and HEK293 cells were seeded in a 96-well plate at 70% confluence, and 4 μg/ml β-galactosidase nanoparticles was added to the medium for X-Gal (5-bromo-4-chloro-3-indolyl-b-D-galactopyranoside, Sigma-Aldrich) staining. The cells were incubated for 12 h in 37°C in a 5% CO2 incubator. After the incubation, the medium was exchanged for DMEM supplemented with 10% FBS for 1 h. The cells were washed twice with PBS and fixed in 4% paraformaldehyde in PBS for 15 min. The fixed cells were reacted with 0.5 mg/mL X-Gal in PBS containing 5 mM $K_4Fe(CN)_6$, 5 mM $K_3Fe(CN)_6$, and 2 mM $MgCl_2$ overnight at 37°C. Bright-field images of the cells were taken with a fluorescence microscope (Olympus IX71, Tokyo, Japan).

α-Galactosidase activity in cells treated with nanoparticles was determined

using a colorimetric assay. Human foreskin fibroblasts were seeded on a 24-well plate at 70% confluency, and nanoparticles in DMEM (4 μg/ml α-galactosidase content in media) were added to the wells and incubated for 24 h at 37°C in a 5% CO2 incubator. After the incubation, the media were exchanged with DMEM supplemented with 10% FBS for 1 h. The cells were washed twice with PBS, and 100 μl of RIPA buffer was added to obtain the cell lysate. After a 10 min room temperature incubation, 10 μl of cell lysate was placed in a 96-well plate and the α-galactosidase assay was performed as described earlier.

## 3.15 Globotriaosylceramide degradation

To examine intracellular Gb3 degradation activity in nanoparticle-treated cells, fibroblasts from a patient with Fabry disease (Coriell Institute for Medical Research, Camden, NJ, USA) were seeded in a 96-well plate and incubated overnight. N-dodecanoyl-NBD-ceramide trihexoside (NBD-Gb3; Abcam, Cambridge, MA, USA), a green-fluorescent Gb3 analog, was added (2 μg/ml in media) and incubated overnight. Then, nanoparticles in DMEM (4 μg/ml α-galactosidase content in media) were added to the wells and incubated for 12 h at 37°C. After the incubation, the cells were washed with PBS. The remaining NBD-GB3 cell fluorescence was measured with a fluorometer (Tecan), and Gb3 degradation was calculated indirectly by subtracting it from initial NBD-GB3 fluorescence.

## 3.16 Statistical analysis

All values are presented as mean ± standard deviation. All experiments were performed in triplicate and compared with the control using the t-test. A p-value $< 0.05$ was considered significant.

# Chapter 4.

# Stabilization of cellular mitochondrial enzyme complex activity through supplementation of 30Kc19 protein

# Chapter 4. Stabilization of cellular mitochondrial enzyme complex activity through supplementation of 30Kc19 protein

## 4.1 Introduction

In the development of industrial mammalian cell culture, it has been an important challenge to maintain the nutrients level and reduce the toxic metabolites during the production process. The nutrient depletion and the accumulation of metabolites result in mitochondrial dysfunction [106-109]. Decreased mitochondrial activity leads to decreased mitochondrial membrane potential (MMP), and eventually decreased ATP production. Low ATP levels cause the down-regulation of “mammalian target of rapamycin” (mTOR) and factors influencing protein translation, leading to lowered specific productivity of recombinant protein [110, 111]. Because hampered mitochondrial activity can also cause mitochondria-mediated apoptosis, maintaining mitochondrial activity is crucial for recombinant protein production in industrial mammalian cell culture [112, 113].

30Kc19 protein (30Kc19) is a major protein of the 30K protein family in silkworm hemolymph. Because anti-apoptotic effects of silkworm hemolymph were observed [1, 2], the potentially beneficial effects of silkworm hemolymph and the 30K proteins were studied [3-5]. In previous study, productivity of EPO was enhanced simultaneously by the expression of 30Kc19 [6, 7]. Although ATP generation was increased by the expression of 30Kc19, it has remained unclear as to how 30Kc19 enhances ATP generation, and thus mitochondrial

function. It was reported that enzyme-stabilizing properties of 30Kc19 [8]. 30Kc19 stabilized various enzymes, such as alkaline phosphatase and horseradish peroxidase, in wide range of environmental conditions. Because activity of enzyme decreases as the enzyme is denatured and becomes chemically changed by surrounding environment [9], stability of enzyme is strongly related with mitochondrial function Thus, It can be hypothesized that increased mitochondrial function with 30Kc19 are due to stabilized enzymes involved in mitochondrial function by 30Kc19. In this study, the effect of recombinant 30Kc19 on the stability of those enzymes in an *in vitro* system was investigated and whether ATP generation of therapeutic proteins enhanced by supplementation of 30Kc19 in a cell culture system.

## 4.2 Effect of 30Kc19 on *in vitro* mitochondrial enzyme stability

Based on the previous results that the mitochondrial membrane potential of CHO cells was increased by the expression of 30Kc19, the effects of 30Kc19 on mitochondrial activity was investigated. For an *in vitro* experiment, mitochondria were isolated from HEK293T cells and added to reaction buffer containing NADH and cytochrome c to examine complex I / III activity. Complex I / III are a group of enzymes that play a central role in electron transfer. In this assay, complex I / III activity was analyzed by measuring the reduction of oxidized cytochrome c. In a time-course analysis, it was demonstrated that the mitochondrial complex I / III reaction was enhanced by 30Kc19 in a dose-dependent manner (Fig. 4.1A). However, mitochondrial

complex I / III activity was not enhanced by 30Kc19 in early stages of the reaction, indicating that 30Kc19 does not enhance initial mitochondrial complex I / III activity but stabilizes long-term activity of the mitochondrial complex I / III (Fig. 4.1B). Thus, these results suggest that the enhancement was due to the stabilization of complex I / III by 30Kc19.

## 4.3 Intracellular and mitochondrial uptake of 30Kc19

Prior to investigate effect 30Kc19 on intracellular enzyme, cellular and mitochondrial uptake of 30Kc19 were observed using western blotting. HeLa cells treated with the 200 μg/ml of 30Kc19 for 1 or 24 h were fractionated and presence of 30Kc19 in mitochondria and cytosol was investigated. Even after 1 h incubation, 30Kc19 was observed not only inside HeLa cell, but also in mitochondria fraction. With 24 h incubation, increased amount of 30Kc19 was observed both cytosol and mitochondria fraction (Fig. 4.2). Because 30Kc19 was able to internalize cells, 30Kc19 was expected to stabilize intracellular enzyme, mitochondrial enzyme complex.

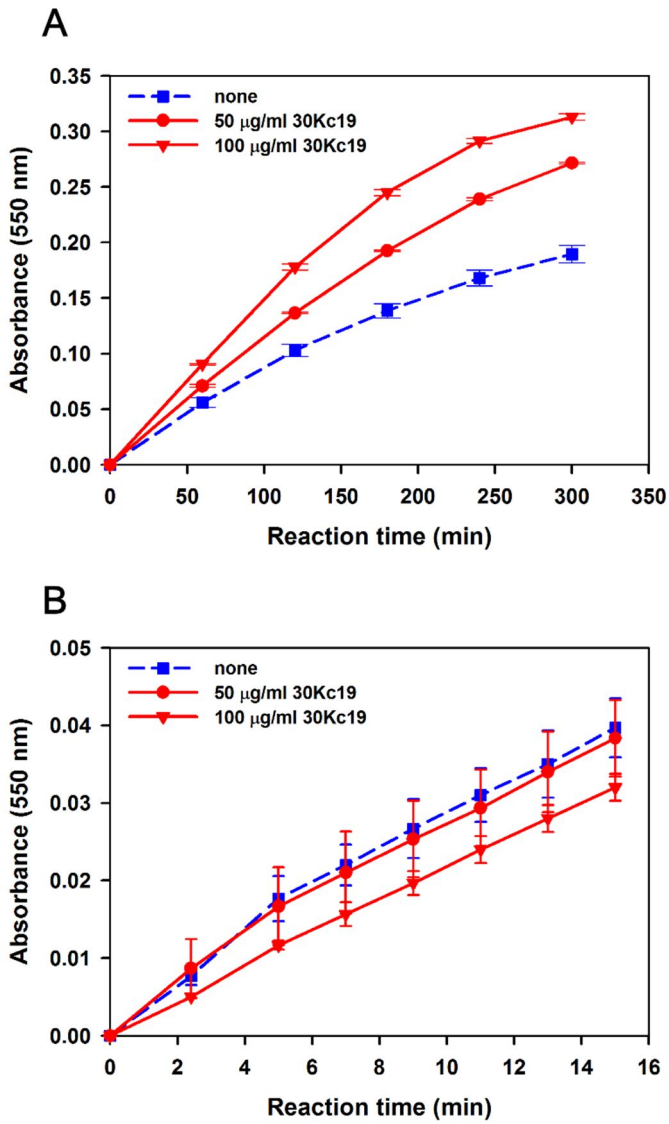


**Figure 4.1** Effects of 30Kc19 on mitochondrial enzyme complex I / III *in vitro* (A) Effect of 30Kc19 on *in vitro* complex I / III activity. (B) At the initial stage of the reaction, 30Kc19 did not affect the activity of complex I /III.

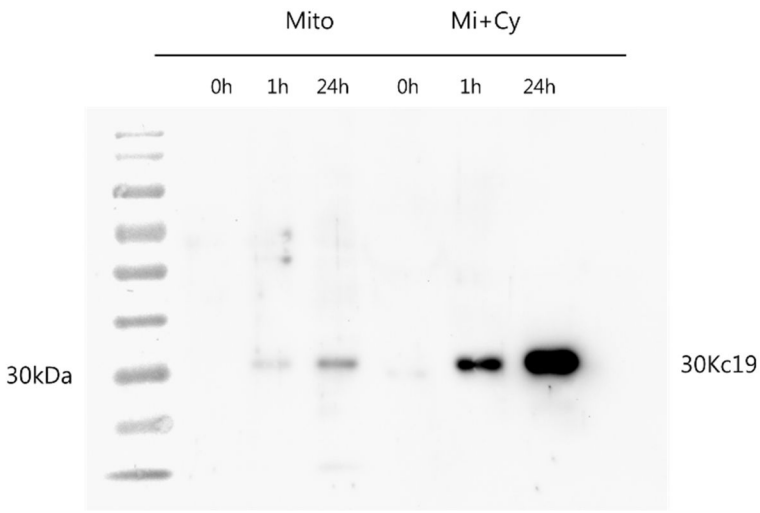


**Figure 4.2** Internalization of 30Kc19 to HeLa cells and mitochondria. HeLa cells were seeded and incubated overnight. Following 1 or 24h incubation with the 200 μg/ml of 30Kc19, cells were detached and subcellular fractionation was performed to separate mitochondria (Mito) and microsomes + cytosol (Mi+Cy) fraction from homogenized cells. And then presence of 30Kc19 in mitochondria and cytosol was investigated by western blotting using 30Kc19 antibody.

## 4.4 Effect of 30Kc19 on intracellular mitochondrial enzyme stability

Based on the *in vitro* results showing enhanced stability mitochondrial enzymes by 30Kc19, the effects of 30Kc19 on the stabilities of intracellular enzymes were studied further.

Intracellular mitochondrial activity was estimated using the MTT assay, a general assay to assess cell viability and mitochondrial activity. In the MTT assay, water-soluble MTT is reduced to a water-insoluble formazan salt by mitochondrial complex II, succinate dehydrogenase [114]. After HeLa cells were cultured with 30Kc19 supplementation for 24 h, the mitochondrial activity was determined using the MTT assay and normalized by cell number. As a result, the normalized mitochondrial activity increased significantly in the 30Kc19-supplemented groups (Fig. 4.3). With 1 mg/ml 30Kc19, mitochondrial activity increased more than 50%.

Together, these results indicate that 30Kc19 improved the stabilities of intracellular enzymes as well as *in vitro*. Recently, a cell-penetrating property of 30Kc19 was demonstrated. Specifically, it was shown that 30Kc19 penetrated into various cell types efficiently and localized in subcellular compartments. Thus, it is supposed that 30Kc19 penetrated into the cells and then stabilized the intracellular enzymes.

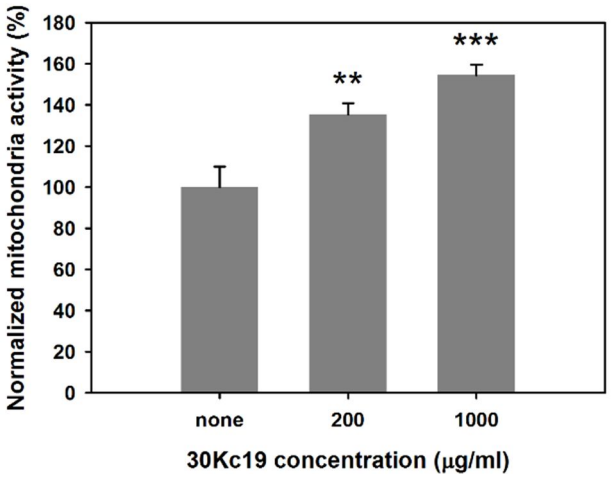


**Figure 4.3** Effects of 30Kc19 on intracellular mitochondrial activity. HeLa cells were seeded and incubated overnight. Following a 24h incubation with the indicated concentrations of 30Kc19, the MTT assay was performed. Each MTT value was normalized by the cell number and represented as a percentage relative to the activity of the 30Kc19-untreated group. *P < 0.05, **P < 0.01 and ***P < 0.005, vs. the 30Kc19-untreated group (n = 3). Error bars indicate SD.

## 4.5 Effect of 30Kc19 on mitochondrial membrane potential and ATP generation

Subsequently, the effects of 30Kc19 on mitochondrial processes were examined. Generally, the improvement of mitochondrial membrane potential (MMP) is accompanied by higher mitochondrial activity. The MMP was analyzed using the fluorescent dye JC-1 [104]. Moreover, because ATP generation is closely related with MMP, the effect of 30Kc19 on ATP generation was also investigated. After a 24h culture of HeLa cells, it was observed that the MMP was increased by supplementation of 30Kc19 (Fig. 4.4A). With 1 mg/ml of 30Kc19 in the medium, MMP increased more than 50%. It was also shown that the intracellular ATP increased with 30Kc19 in a dose-dependent manner (Fig. 4.4B). All these results indicate that 30Kc19 improved MMP and ATP generation via stabilization of mitochondrial enzyme activities.

## 4.6 Conclusions

In this work, it was demonstrated that 30Kc19 stabilized the mitochondrial enzyme complex *in vitro*, which are related to protein productivity in industrial mammalian cell culture. Furthermore, intracellular enzyme stability was increased by adding 30Kc19 to the culture medium. In conclusion, 30Kc19 is anticipated to be a useful tool for the both quantity and quality improvement of recombinant protein production in industrial mammalian cell culture.

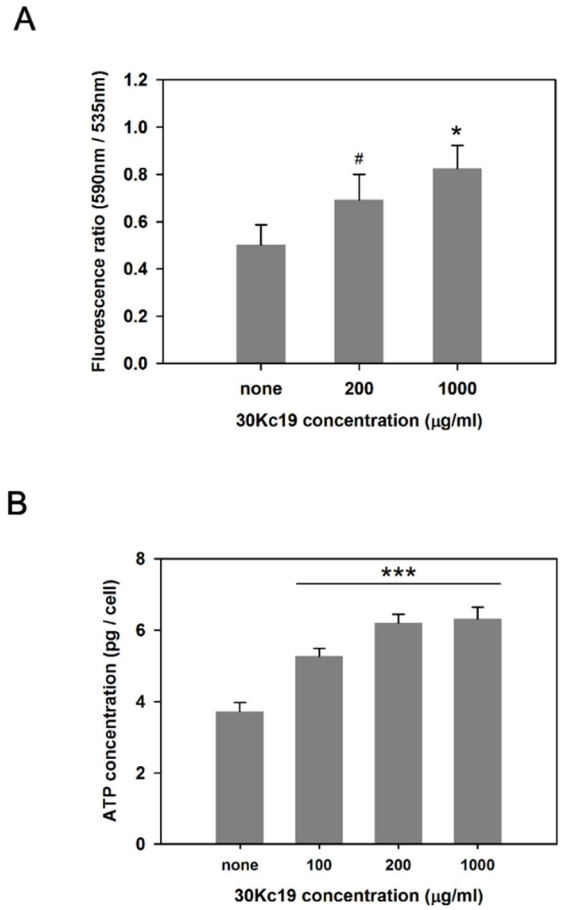


**Figure 4.4** Enhancement of mitochondrial metabolism by 30Kc19 (A) Effect of 30Kc19 on the mitochondrial membrane potential (MMP) of HeLa cells. MMP was estimated using JC-1 and represented as a ratio of emission fluorescence (590 / 535 nm). (B) Effect of 30Kc19 on ATP generation in HeLa cells. The ATP content in each sample was measured using an ATP bioluminescent somatic cell assay kit. Each ATP concentration was normalized by the cell concentration. #$P < 0.1$, *$P < 0.05$ and ***$P < 0.005$, vs. the 30Kc19-untreated group ($n = 3$). Error bars indicate SD.

# Chapter 5.

# Synthesis of protein nanoparticles using 30Kc19 protein and human serum albumin

# Chapter 5. Synthesis of protein nanoparticles using 30Kc19 protein and human serum albumin

## 5.1 Introduction

Drug delivery using nano-sized carriers is a rapidly growing research field since recent studies on nanotechnology led to the synthesis of uniformly sized, well dispersed, and non-cytotoxic nanoparticles. Various therapeutic cargos such as drugs, DNA, and proteins can be loaded onto the surface of solid nanoparticles or inside a matrix of polymeric nanoparticles [115-117]. Between the two approaches, immobilizing nanoparticles inside a matrix of polymeric nanoparticles improves stability of the cargo as the cargo is protected within the nanoparticle matrix rather than being placed on the nanoparticle surface [118]. Drug carriers loaded with cargo should have controlled and sustained drug-releasing ability to achieve successful delivery of the therapeutic cargo. Among diverse polymeric nanoparticles, protein-based nanoparticles have advantages such as non-cytotoxicity, ease of preparation, sustained release, and covalent modifications due to their abundant functional groups [13, 119].

Diverse nanoparticles have been applied to drug delivery, as nanocarrier protect cargo from degradation and enhance intracellular penetration [53]. Among various nanoparticles, polymeric nanoparticles have an additional advantage of protecting therapeutic cargo located inside. Protein is a suitable polymeric material for nanocarrier, as it has beneficial features such as non-toxicity and biodegradability [118].

Albumin is the most actively studied protein because it is a FDA-approved

material for therapeutic use. Albumin has abundant functional groups to bind with cargo, and can be modified with ligands [59, 60]. Albumin has its own endocytosis route mediated by gp60, an albumin receptor located at caveolae. However, some cells lack or have a limited number of caveolae; thus, additional ligands are desirable to efficiently deliver albumin nanoparticles loaded with therapeutic agents into target cells. Maintaining drug cargo activity is also challenging, as enzyme cargo can be deactivated during the nanoparticle preparation process or after intracellular delivery. Cell penetrating peptides and various target-specific ligands have been applied to albumin nanoparticles to enhance delivery [60, 96, 120]; but there are only a few studies have actually enhanced cargo stability, particularly that for therapeutic enzymes. In this study, the recombinant 30Kc19 protein, originating from silkworm, was used with albumin to prepare nanoparticles in order to enhance both cellular uptake and cargo stability.

The 30Kc19 protein is a member of the 30K protein family, and similarly structured proteins are found in silkworm hemolymph. 30Kc19 is the most abundant protein among 30K proteins with molecular weights of about 30 kDa. In previous studies, 30K proteins exhibited anti-apoptotic effect in various cells by gene expression or addition of 30K proteins in recombinant form produced from *Escherichia coli* [1-7, 121-123]. The cell-penetrating and enzyme-stabilizing effects of the 30Kc19 protein have also been observed in recent studies [124]. 30Kc19 protein-human serum albumin (HSA) hybrid protein nanoparticles were used for the first time to enhance uptake and intracellular stability of an enzyme cargo. In this study, 30Kc19-HSA nanoparticles were prepared and characterized, and cellular toxicity and uptake were examined to

observe the effect of the 30Kc19 protein on the protein nanoparticles.

## 5.2 Preparation and characterization of 30Kc19-HSA nanoparticles

Among various methods, desolvation method is widely used for preparation of protein nanoparticles because of its simple process [125]. Initially, proteins are stably hydrated in aqueous solution. As desolvation regent (e.g., ethanol, methanol, and acetone) added dropwise to aqueous solution, proteins are gradually detached from water molecules. At certain point, proteins aggregate into a controlled and uniform size. Then Protein aggregates are stabilized using a crosslinking agent (e.g., glutaraldehyde) crosslinking superficial free amine groups of aggregates (Fig. 5.1) [96]. At first, preparation of 30Kc19 protein nanoparticles was attempted using desolvation method. However, nanoparticles using only 30Kc19 protein were unstable; it aggregated excessively and precipitated in PBS and cell culture media. Hence, 30Kc19-HSA hybrid nanoparticles were prepared to secure both beneficial effect of 30Kc19 protein and structural stability of nanoparticles.

The nanoparticles were prepared with two initial pH of aqueous solution, considered one of critical parameter in preparation of protein nanoparticles, with 0 (HSA only) and 50 wt.% 30Kc19 protein. ELS spectrophotometry was used to investigate the size, polydispersity, and zeta potential of HSA and 50 wt.% 30Kc19-HSA protein nanoparticles. HSA nanoparticles had no difference in size with pH change of aqueous protein solution. On the other hand, mean size of 50% 30Kc19 nanoparticles was significantly decreased with pH change;

279.0 nm to 144.0 nm. Because 100% 30Kc19 nanoparticles were aggregated too high and unstable, size decrease with preparation at high pH suggested 50% 30Kc19-HSA nanoparticles synthesized more stably in that condition (Fig. 5.2A). Both HSA and 50% 30Kc19 nanoparticles had showed similar polydispersity, ~0.1. Because polydispersity index that less than 0.2 considered monodisperse (uniform size), the result suggested that nanoparticles were synthesized in uniform size. The zeta potential of the HSA nanoparticles showed negligible difference with change of pH of initial protein solution, as observed in nanoparticles size, while that of 50% 30Kc19-HSA nanoparticles exhibited increased zeta potential in absolute value (Fig. 5.2B). Because absolute value of zeta potential corresponds with stable dispersion in buffer or culture media, higher pH of initial protein solution would be regarded as appropriate condition for 50% 30Kc19-HSA nanoparticles. SEM images were obtained to evaluate nanoparticle morphology (Fig. 5.2C). HSA nanoparticles had rigid, uniform spherical morphology regardless of initial protein solution pH. In contrast, 30Kc19-HSA nanoparticles exhibit morphological difference pH condition. In synthesis with normal pH, aggregated and instable morphology were observed. However, with high pH 50% 30Kc19-HSA nanoparticles exhibit stable and uniform morphology similar to HSA nanoparticles. These results were corresponding with size and zeta potential data obtained using ELS. The protein charge would play important role when protein aggregate in controlled manner. Since HSA has lower pI value (~ 4) compared with 30Kc19 (~ 7), higher pH of protein solution might be required for 30Kc19 protein to secure sufficient charge for stable formation of nanoparticles.

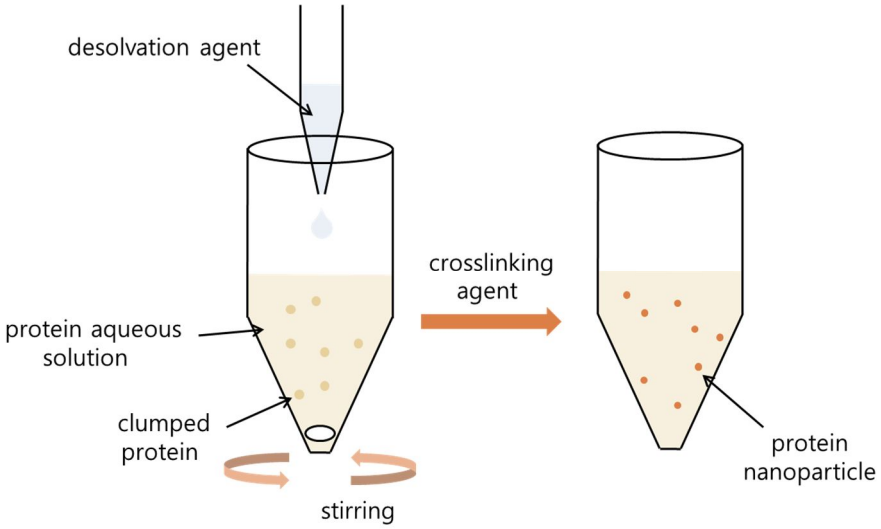


**Figure 5.1** Schematic diagram of protein nanoparticles preparation.

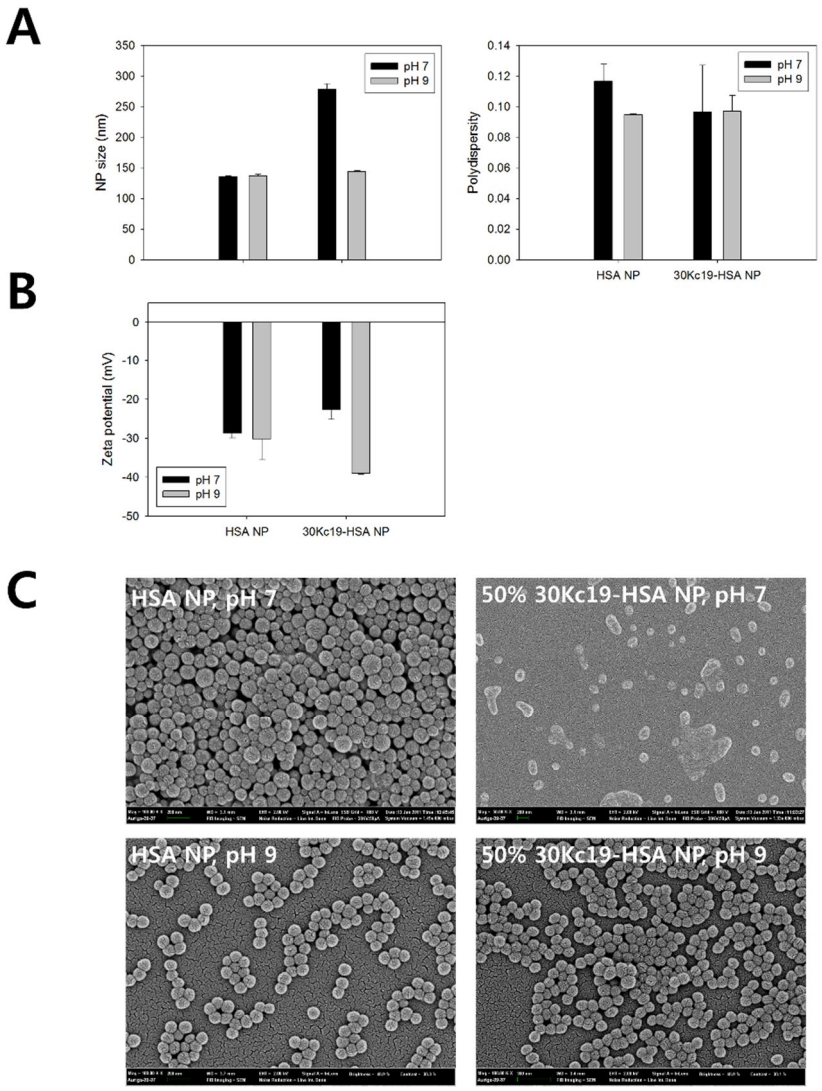


**Figure 5.2** Characterization of the prepared 30Kc19-HSA nanoparticles. (A) Nanoparticle size and polydispersity of the 30Kc19 protein in the nanoparticles as measured by electrophoretic light scattering spectrophotometry (ELS). The nanoparticles were resuspended in distilled water. (B) Zeta potential changes of the nanoparticles measured by ELS. (C) SEM images of the nanoparticles (magnification, ×2000).

## 5.3 Cellular toxicity of 30Kc19-HSA nanoparticles

The stably prepared and characterized HSA and 30Kc19-HSA nanoparticles were added to HeLa cells to investigate cellular toxicity. The non-cytotoxicity of protein nanoparticles is one of advantages over other metal or polymer nanoparticles. When metal nanoparticles internalized into cells via endocytosis, the metal ion eluted from nanoparticles in low-pH lysosomes. In particular, it is the main challenge of nanoparticles based on heavy metal, e.g. quantum dots. On the other hand, the proteins consisting protein nanoparticles are degraded easily by proteases inside cells. Moreover, HSA is widely used in biological field since it has approved by the FDA for pharmaceutical applications because of its non-cytotoxicity [126]. It was also previously shown that 30Kc19 protein exhibits neither cytotoxicity nor immunogenicity issues in mice [124]; thus, it was expected that the protein nanoparticles produced from these two proteins would also not be toxic to cells. The MTT assay was used to assess nanoparticle toxicity. No significant decrease in MTT was observed in HeLa cells treated with 30Kc19-HSA nanoparticles, indicating negligible cellular toxicity (Fig. 5.3). It suggests that 30Kc10-HSA nanoparticles would be applied for cellular delivery, while further *in vivo* toxicity should be tested.

## 5.4 Cellular uptake of 30Kc19-HSA nanoparticles

Confocal microscope images of HeLa and HEK293 cell treated with HSA and 50% 30Kc19-HSA nanoparticles were taken to visualize uptake of nanoparticles. After a 24 h treatment, HSA and 30Kc19-HSA nanoparticles

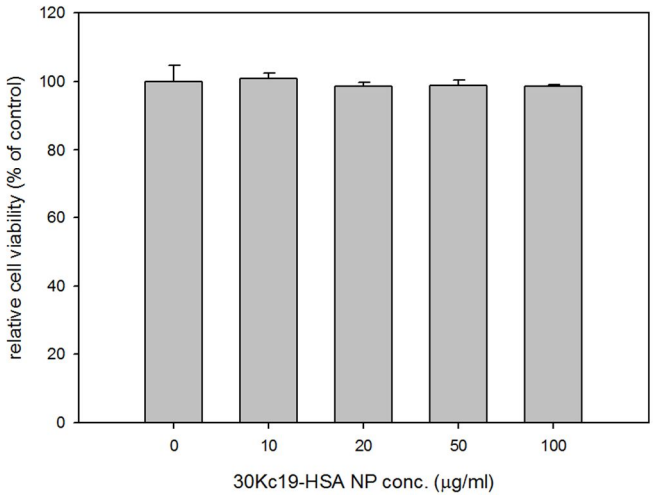


**Figure 5.3** Cellular toxicity of 30Kc19-HSA nanoparticle. HeLa cells treated with 0-100 µg/ml of 30Kc19-HSA nanoparticles for 24 h. Cellular toxicity was measured using MTT assay.

were found in the cytoplasm (Fig. 5.4). Internalized nanoparticles were localized in punctuate forms, suggesting a possible nanoparticle entrapment in endosomes inside cells. In HeLa cells, 50% 30Kc10-HSA nanoparticles exhibit similar fluorescence compared with HSA nanoparticles. However, higher fluorescence was observed in HEK293 cells treated with 30Kc19-HSA nanoparticles than with HSA nanoparticles. In HeLa cells, HSA nanoparticles uptake is benefited by caveolae-mediated endocytosis. On the other hand, HEK293 cell has very little caveolae and cellular uptake of HSA nanoparticles were limited. However, because the 30Kc19 protein exhibits cell-penetrating ability, as shown in previous study [124], cellular uptake of the 30Kc19-HSA nanoparticles would benefit from the 30Kc19 protein and exhibited higher cellular uptake in HEK293 cells.

## 5.5 Conclusions

In this work, protein nanoparticles using 30Kc19 protein were produced and characterized. 30Kc19 and HSA were used as building block of protein nanoparticles to exploit both beneficial effect of 30Kc19 protein stability of HSA nanoparticles. 50 wt.% 30Kc19-HSA nanoparticles were successfully prepared in basic condition, with uniform spherical morphology and stable dispersion in buffer and culture media. 30Kc19-HSA nanoparticles showed negligible toxicity when treated to HeLa cells. 30Kc19-HSA nanoparticles also exhibited increase in cellular uptake when compared with HSA nanoparticles, particularly in caveolae-lacking cells.

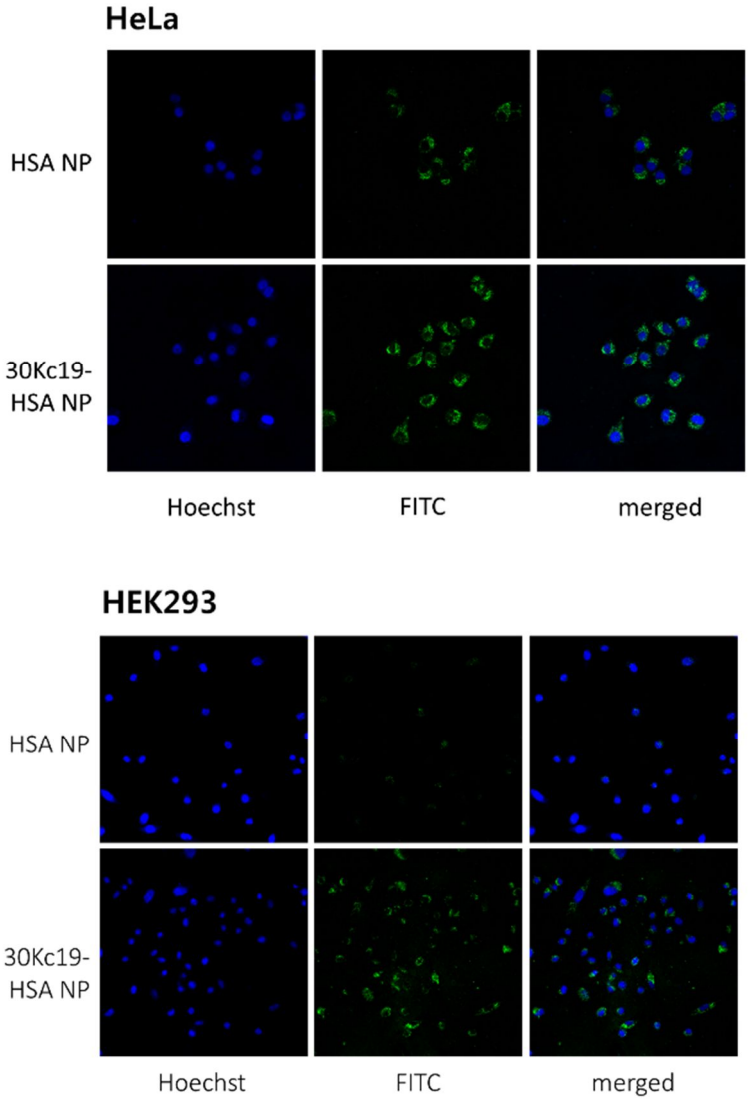


**Figure 5.4** Cellular uptake of HSA and 30Kc19-HSA nanoparticles. Confocal microscopic image of HeLa and HEK293 cells treated with 100 μg/ml HSA or 30Kc19-HSA nanoparticles for 24 h. The nanoparticles were labeled with FITC (green fluorescence) and nuclei were stained with Hoechst 33342 (blue fluorescence).

# Chapter 6.

# Protein nanoparticles for protein cargo delivery using 30Kc19 protein and human serum albumin

# Chapter 6. Protein nanoparticles for protein cargo delivery using 30Kc19 protein and human serum albumin

## 6.1 Introduction

Albumin is an actively studied protein for preparing protein nano-carriers, as it is biodegradable, and nontoxic and non-immunogenic *in vivo*. Albumin has diverse drug binding sites and many charged amino acids, allowing efficient loading of charged drugs, oligonucleotides, or proteins. Therapeutic cargo can be easily loaded in a matrix of albumin nanoparticles without an additional reaction. Albumin nanoparticles can be modified further by drug targeting ligands using functional groups on the nanoparticle surface [59, 60]. In addition, albumin is commercially available in large quantities and can be prepared simply in a moderate condition, which is suitable for mass production of a drug delivery carrier [14]. Because albumin can be internalized into cells via the endocytosis-mediated albumin receptor located at caveolae, albumin nanoparticles can also utilize this cellular uptake route. However, additional ways to enhance albumin nanoparticle uptake are needed because some cells lack or have limited caveolae. Furthermore, the activity of drug cargo, particularly enzymes, is vulnerable to solvents during nanoparticle preparation and to intracellular proteases after delivery to cells. In this study, a recombinant 30Kc19 protein originating from silkworm was used with albumin nanoparticles to resolve cellular uptake and cargo stability issues.

The 30Kc19 protein is a member of the 30K protein family, and similarly

structured proteins are found in silkworm hemolymph. 30Kc19 is the most abundant protein among 30K proteins with molecular weights of about 30 kDa. In previous studies, 30K proteins exhibited anti-apoptotic effect in various cells by gene expression or addition of 30K proteins in recombinant form produced from *Escherichia coli* [10-20]. The cell-penetrating and enzyme-stabilizing effects of the 30Kc19 protein have also been observed in recent studies [21]. 30Kc19 protein-human serum albumin (HSA) hybrid protein nanoparticles were used to enhance uptake and intracellular stability of an enzyme cargo. In this study, 30Kc19-HSA nanoparticles loaded with β-galactosidase were prepared and characterized, and cellular uptake and intracellular enzyme cargo activity of nanoparticles with various 30Kc19 concentrations were examined to observe the effect of the 30Kc19 protein on the protein nanoparticles.

## 6.2 Characterization of β-gal-loaded 30Kc19-HSA nanoparticles

The 30Kc19-HSA protein nanoparticles were prepared using the desolvation method, which is a well-developed procedure to form protein nanoparticles [22]. Desolvation is a process where proteins in aqueous solution aggregate into a controlled and uniform size when ethanol is added drop wise. Protein aggregates loaded with cargo such as chemicals, DNA plasmids, or therapeutic proteins are stabilized using a crosslinking agent (glutaraldehyde) [23]. In this study, β-galactosidase was selected as the model therapeutic cargo protein, for convenience in assessing activity. The production of protein nanoparticles and

loading of β-galactosidase onto the nanoparticles were performed simultaneously in an identical reaction vessel by adding enzyme to an aqueous solution of HSA and/or 30Kc19 protein (Fig. 6.1).

ELS spectrophotometry was used to investigate the effect of the 30Kc19 protein on size, polydispersity, and zeta potential of the protein nanoparticles. The sizes of the prepared nanoparticle were 170–350 nm, showing a tendency to increase in size with an increase in wt.% of the 30Kc19 protein. The polydispersity of the nanoparticles also increased with the proportion of 30Kc19 in protein solution, suggesting a decrease in uniformness for nanoparticles containing a higher 30Kc19 wt.% (Fig. 6.2A). The zeta potential of the 30Kc19-HSA nanoparticles was −20 to −30 mV at neutral pH (Fig. 6.2B). The zeta potential corresponded with the observed stable dispersion of nanoparticles in water, PBS buffer, and cell culture media (data not shown). SEM images were obtained to evaluate the effect of the 30Kc19 protein on nanoparticle morphology (Fig. 6.2C). The mean size and size variation of the nanoparticles increased with the wt.% of the 30Kc19 protein in the nanoparticles. The nanoparticles had a uniform and rigid spherical shape from 0% to 50% 30Kc19 nanoparticles. However, when the wt.% of 30Kc19 protein exceeded 50%, the nanoparticles exhibited a distorted shape and tended to stick to one another. Extremely small (<5 nm) nanoparticles were observed with a high wt.% of 30Kc19 (>70%), particularly at 100 wt.% The decreased mean nanoparticle size in 100 wt.% 30Kc19 seemed to be due to the high proportion of these tiny particles.

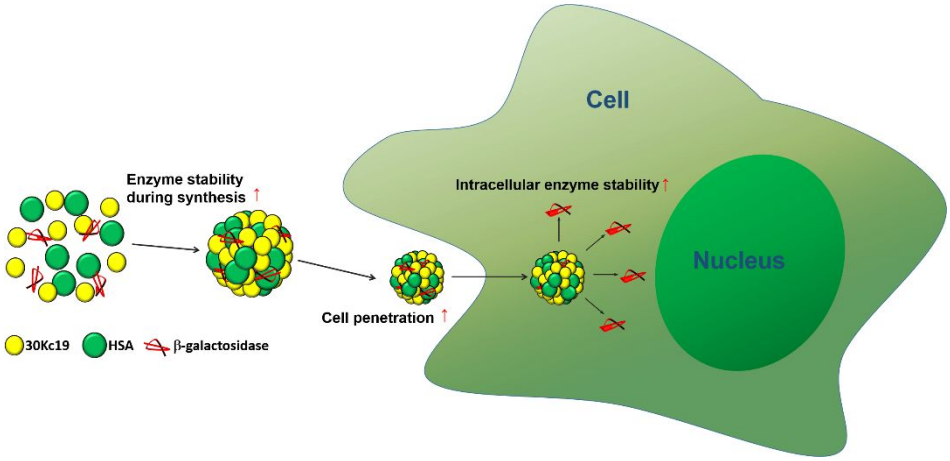


**Figure 6.1** A schematic illustration for the intracellular delivery of enzyme cargo by the 30Kc19-HSA nanoparticles.

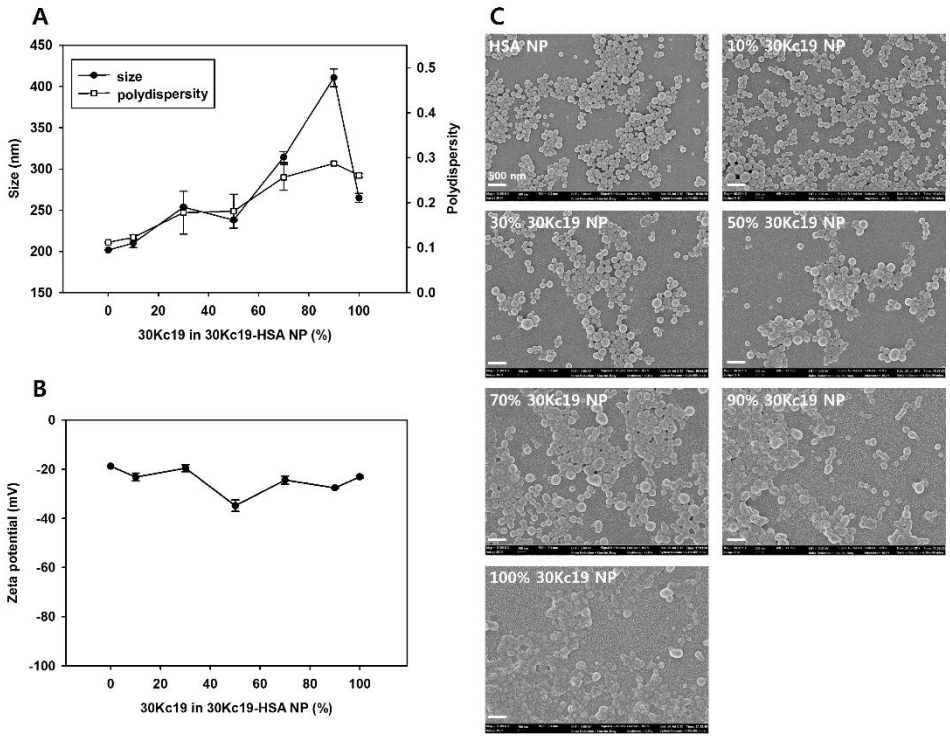


**Figure 6.2** Characterization of the prepared 30Kc19-HSA nanoparticles. (A) Nanoparticle size and polydispersity vs. wt.% of the 30Kc19 protein in the nanoparticles as measured by electrophoretic light scattering spectrophotometry (ELS). The nanoparticles were resuspended in distilled water. (B) Zeta potential changes of the 30c19 nanoparticles measured by ELS. (C) SEM images of the 30Kc19-HSA nanoparticles containing 0–100 wt.% of the 30Kc19 protein (magnification, ×2000).

## 6.3 β-Galactosidase loading and *in vitro* release of 30Kc19-HSA nanoparticles

β-Galactosidase loading efficiency was assessed indirectly using the fluorescently labeled enzyme remaining in the supernatant of the reaction solution (Fig. 6.3A). β-Galactosidase was loaded onto the nanoparticles with a yield of 80–95%, and slightly higher enzyme loading was observed as the wt.% of 30Kc19 increased in the nanoparticles. Activity of the remaining enzyme was measured using a colorimetric assay (Fig. 6.3B). The specific activity of the β-galactosidase remaining in the supernatant increased with increasing 30Kc19 content in the nanoparticles up to 50%. The remaining enzyme exhibited a decrease in specific activity in the nanoparticle supernatant with a 30Kc19 ratio > 50%.

The fluorescence of the released β-galactosidase was measured to assess the release efficiency of the loaded enzyme from nanoparticles (Fig. 6.4A). At all ratios of 30Kc19, 30–50% of the loaded β-galactosidase was released from the nanoparticles within the first 24 h. Then, sustained release was observed for > 200 h. The release of β-galactosidase increased with increasing 30Kc19 ratio in the nanoparticles up to 50%, whereas nanoparticles containing > 70% 30Kc19 exhibited a decrease in release with increasing 30Kc19 ratio. The activity of the released β-galactosidase was also measured using a colorimetric activity assay (Fig. 6.4B). β-Galactosidase released from 50% 30Kc19 showed the highest specific activity, suggesting that 50% is the optimal percent for enzyme delivery.

Previous results showed that the 30Kc19 protein has enzyme stabilizing

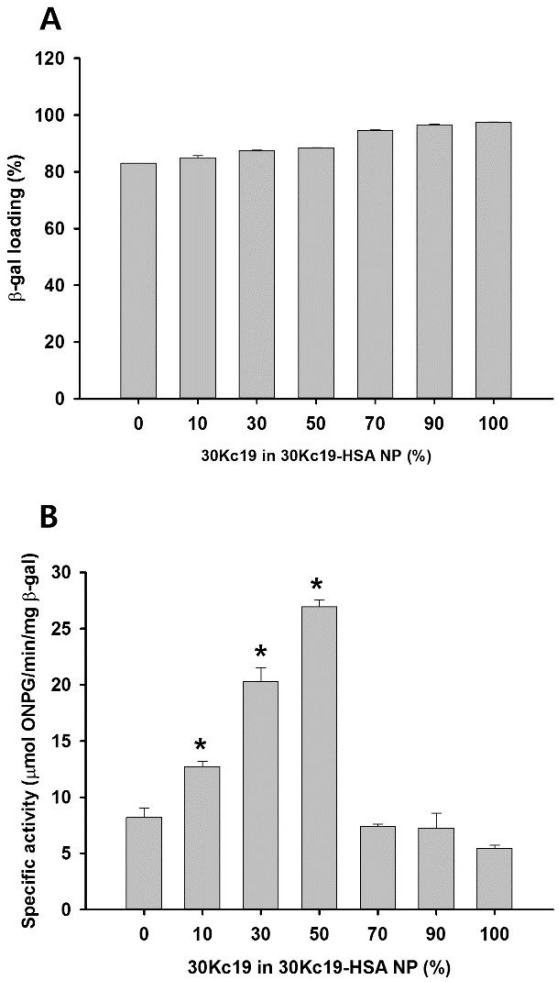


**Figure 6.3** The enzyme loading efficiency and enzyme stabilizing effect of the 30Kc19 during preparation of the nanoparticles. (A) β-galactosidase loading efficiency of the 30Kc19-HSA nanoparticles with increasing wt.% (0–100%) of the 30Kc19 protein, assessed indirectly using the fluorescent-labeled enzyme remaining in the supernatant of the reaction solution. (B) The specific activity of the remaining β-galactosidase in preparation of the 30Kc19-HSA nanoparticles assessed using β-galactosidase activity assay (*$p < 0.05$).

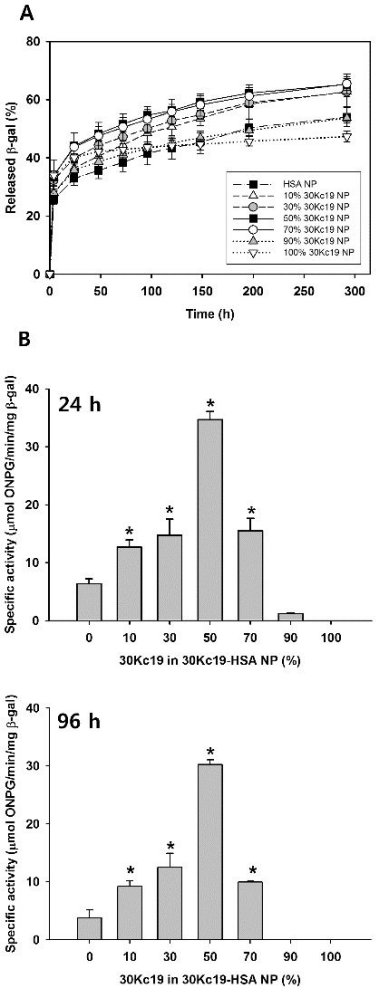


**Figure 6.4** *in vitro enzyme releases* of the 30Kc19-HSA nanoparticles. (A) *In vitro* release profile of nanoparticles containing 0–100 wt.% of the 30Kc19 protein. The β-galactosidase released was isolated from the nanoparticles by centrifugation at 12000 × g and measured by assessing fluorescent label. (B) Specific activity of β-galactosidase released from the nanoparticles. The β-galactosidase released after a 24 h and 96 h incubation was collected and measured by the ONPG colorimetric assay (*$p < 0.05$).

activity [24]; hence, higher β-galactosidase activity was expected as the 30Kc19 protein ratio in the nanoparticles increased. In contrast, the higher amount of 30Kc19 protein in the nanoparticles destabilized the structure of the protein nanoparticles compared with that of the HSA nanoparticles, indicating that a balance in the amount of 30Kc19 added to the nanoparticles is a key to provide the highest β-galactosidase stability while retaining the shape and function of the nanoparticles. Based on the data, β-galactosidase activity in the nanoparticles had an optimum 50 wt.% of 30Kc19 protein content. Nanoparticles containing > 70 wt.% of the 30Kc19 protein were excluded from further experiments due to destabilized structure and low β-galactosidase activity.

## 6.4 Cellular toxicity of 30Kc19-HSA nanoparticles loaded with β-Galactosidase

The characterized 30Kc19-HSA nanoparticles were added to animal cells to investigate cellular toxicity. HSA has been approved by the FDA for pharmaceutical applications because of its non-cytotoxicity [25], and it was previously shown that 30Kc19 protein exhibits neither cytotoxicity nor immunogenicity issues in mice. [21]; thus, it was expected that the protein nanoparticles produced from these two proteins would also not be toxic to cells. The MTT assay was used to assess nanoparticle toxicity. No significant decrease in MTT was observed in HeLa and HEK293 cells treated with 30Kc19-HSA nanoparticles, indicating negligible cellular toxicity (Fig. 6.5).

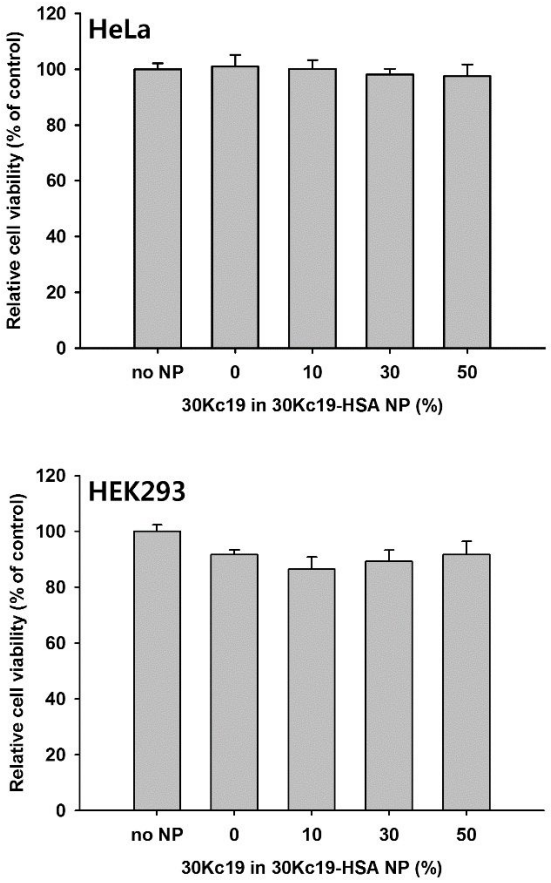


**Figure 6.5** MTT assay of HeLa and HEK293 cells treated with 200 μg/ml of 30Kc19-HSA nanoparticles containing 0–50 wt.% of the 30Kc19 protein for 24 h.

## 6.5 Cellular uptake of 30Kc19-HSA nanoparticles loaded with β-Galactosidase

Effective cellular uptake of the nano carrier is essential for drug delivery. Confocal microscope images of HeLa and HEK293 cell treated with 30Kc19-HSA nanoparticles were taken to visualize uptake of nanoparticles. After a 24 h treatment, HSA and 30Kc19-HSA nanoparticles were found in the cytoplasm (Fig. 6.6A). Internalized nanoparticles were localized in punctuate forms, suggesting a possible nanoparticle entrapment in endosomes inside cells. However, further experiments using endolysosomal marker would be needed to confirm whether nanoparticles were trapped in endosomes. Higher fluorescence was observed in cells treated with nanoparticles containing the 30Kc19 protein than with HSA only nanoparticles. Because the 30Kc19 protein exhibits cell-penetrating ability, as shown in previous study [21], cellular uptake of the 30Kc19-HSA nanoparticles would benefit from the 30Kc19 protein. A flow cytometry analysis was carried out to quantitatively assess nanoparticle uptake into the cells (Fig. 6.6B). The fluorescence peaks shifted significantly from the negative control peak in both HeLa and HEK293 cells, indicating that the HSA and 30Kc19-HSA nanoparticles were internalized into the cells. Cells treated with the 30Kc19-HSA nanoparticles exhibited higher fluorescence intensity inside cells compared with that of the HSA nanoparticles. The mean fluorescence intensity (MFI) shifted from 13.0 to 15.3 in HeLa cells and from 26.5 to 39.8 in HEK293 cells.

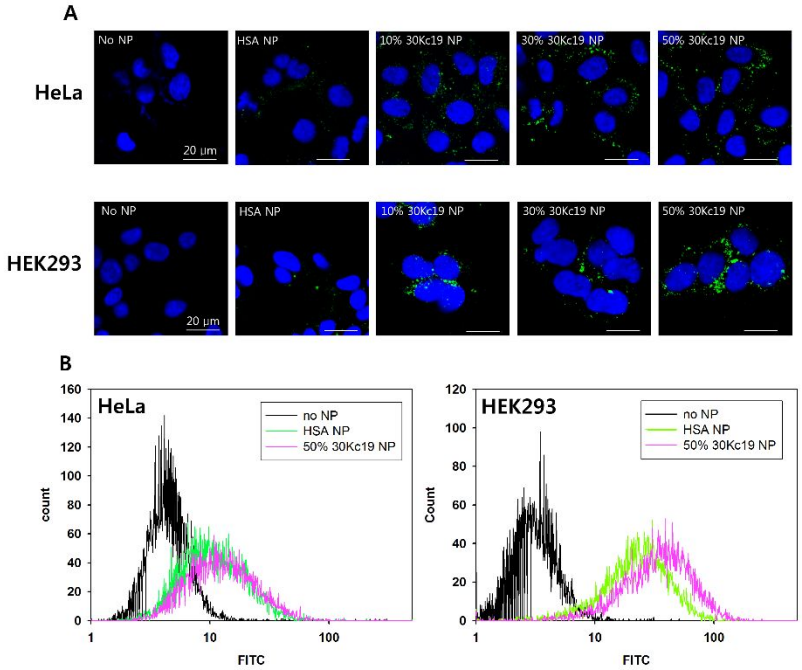


**Figure 6.6** Cellular uptake of 30Kc19-HSA nanoparticles. (A) Confocal microscopic image of HeLa and HEK293 cells treated with 200 μg/ml 30Kc19-HSA nanoparticles containing 0–50 wt.% of the 30Kc19 protein for 24 h. The nanoparticles were labeled with Alexa Fluor® 488 (green fluorescence) and nuclei were stained with Hoechst 33342 (blue fluorescence). (B) Flow cytometry analysis of HeLa and HEK293 cells treated with HSA or 30Kc19-HSA nanoparticles. Cells on 24-well plate were treated with Alexa Fluor® 488-labeled protein nanoparticles for 12 h, washed with PBS twice, and detached from the well using 0.25% trypsin-EDTA, then collected and further washed with PBS. Alexa Fluor® 488-positive cells were detected using a FACSAria II. Fluorescence intensity is shown as a log scale.

## 6.6 Intracellular β-galactosidase activity delivered by nanoparticles

HeLa and HEK293 cells were treated with 30Kc19-HSA nanoparticles, and β-galactosidase activity of the cell lysate was assayed using a colorimetric method to investigate the intracellular β-galactosidase activity that was delivered (Fig. 6.7). Cells treated with 30Kc19-HSA nanoparticles showed higher intracellular β-galactosidase activity compared with that of the HSA nanoparticles. Enzyme activity increased drastically with the wt.% of the 30Kc19 protein in the nanoparticles. Intracellular β-galactosidase activity in HEK293 cells treated with 50 wt.% 30Kc19 nanoparticles for 24 h increased by more than five-fold compared with that in HSA nanoparticle-treated cells. β-Galactosidase activity remained higher for 30Kc19-HSA than that for the HSA-only protein nanoparticles when cells were incubated for an additional 72 h after being washed with fresh media. Intracellular β-galactosidase activity was also visualized in situ by X-gal staining (Fig. 6.8). Both cell types treated with 30Kc19-HSA nanoparticles exhibited higher intracellular enzyme activity compared with that of the HSA nanoparticles, coinciding with the cell lysate result shown above.

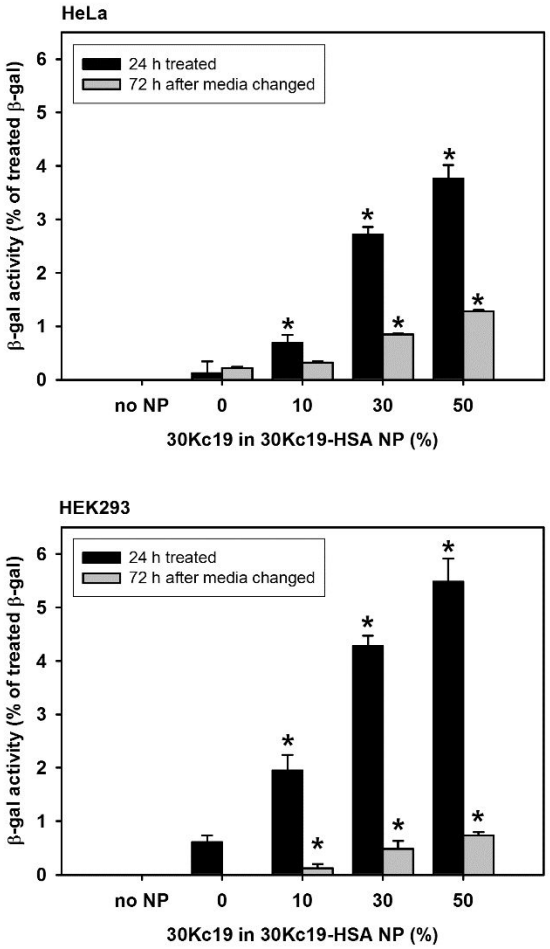


**Figure 6.7** Quantitative analysis of β-galactosidase activity in HeLa and HEK293 cells treated with 30Kc19-HSA nanoparticles containing 0–50 wt.% of the 30Kc19 protein (4 μg/ml β-galactosidase content in media, 24 h). Intracellular β-galactosidase activity of the cells was measured immediately after the 24 h incubation or an additional incubation for 72 h after a fresh media change (*$p < 0.05$).

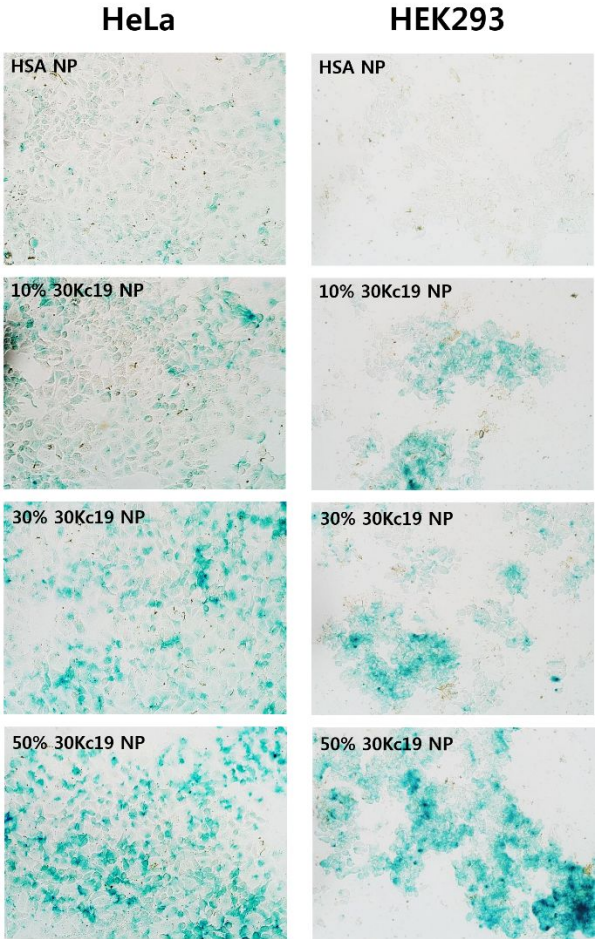


**Figure 6.8** β-Galactosidase activity of HeLa and HEK293 cells assessed by X-gal staining. HeLa and HEK293 cells treated with the 30Kc19-HSA nanoparticles containing 0–50 wt.% of 30Kc19 (4 μg/ml β-galactosidase content in media, 24 h). Blue color developed due to X-gal staining.

## 6.7 Conclusions

The 30Kc19 protein, which has the ability to penetrate cells and stabilize enzymes, was used with HSA as a protein nanoparticle building block loaded with β-galactosidase for cellular delivery. Nanoparticles made from the 30Kc19 protein and HSA were spherical in shape with uniform size and high β-galactosidase loading efficiency. The β-galactosidase loaded on 30Kc19-HSA nanoparticles was released in a sustained manner, and β-galactosidase released from the 30Kc19-HSA nanoparticles had more stabilized enzyme activity than that from HSA nanoparticles. The 30Kc19-HSA nanoparticles also exhibited enhanced cellular uptake and β-galactosidase activity when compared with the HSA nanoparticles. 30Kc19-HSA protein nanoparticles are expected to be used as a versatile tool for intracellular delivery of therapeutic proteins, particularly enzyme replacement therapy for lysosomal disorders such as Fabry disease and Gosher disease. Furthermore, these nanoparticles will be useful as a specific anti-cancer drug delivery vehicle when combined with cell targeting ligands.

# Chapter 7.

# Protein nanoparticles for therapeutic protein delivery using 30Kc19 protein and human serum albumin

# Chapter 7. Protein nanoparticles for therapeutic protein delivery using 30Kc19 protein and human serum albumin

## 7.1 Introduction

Fabry disease is a rare X-linked disorder of lysosomal storage caused by α-galactosidase deficiency [127]. As α-galactosidase hydrolyzes neutral glycosphingolipids in lysosomes, lack of this enzyme results in accumulation of glycosphingolipids, mainly globotriaosylceramide (Gb3), in various tissues, causing multi-organ dysfunction and possible premature death. Enzyme replacement therapy (ERT) is the only treatment available for lysosomal disorders like Fabry disease [128]. Commercial recombinant human α-galactosidase (e.g., Fabrazyme) is used for ERT in patients with Fabry disease. However, administered α-galactosidase was shown vulnerability to clearance from blood by liver and kidney and degradation by proteases and immune reaction *in vivo* [129]. Furthermore, as the cost of commercial α-galactosidase for ERT is very high, an appropriate drug delivery system to effectively treat Fabry disease is required [130].

In previous studies, an anti-apoptotic effect was observed in various cell types via 30K gene expression or after adding recombinant 30K protein produced from *Escherichia coli* [1-7, 121-123, 131]. Moreover, the cell-penetrating and enzyme-stabilizing effects of the 30Kc19 protein were also observed in recent studies [8, 124]. Thus, the 30Kc19 protein is suitable to enhance cellular uptake and stabilize drug cargo activity; hence, 30Kc19 protein-human serum albumin

(HSA) hybrid protein nanoparticles were synthesized. These 30Kc19-HSA nanoparticles enhance cellular uptake and intracellular stability of model enzyme. In this study, the 30Kc19-HSA nanoparticles were loaded with α-galactosidase, the therapeutic enzyme to treat Fabry disease, and were prepared and characterized. Then, cellular uptake, intracellular enzyme cargo activity, and globotriaosylceramide (Gb3) degradation were examined using 30Kc19-HSA nanoparticles loaded with α-galactosidase.

## 7.2 Production and characterization of 30Kc19-HSA nanoparticles

The 30Kc19-HSA protein nanoparticles were prepared by the desolvation method [132]. In this process, ethanol is added dropwise to an aqueous solution containing HSA, the 30Kc19 protein, and α-galactosidase. As dehydration occurs gradually due to the ethanol, protein molecules lose their stable hydrated conformation and aggregate with neighboring molecules. This aggregation occurs in a controlled uniform size under appropriate conditions. Then, the aggregated protein nanoparticles were stabilized using a crosslinking agent (e.g. glutaraldehyde) [96]. Size, polydispersity, and zeta potential of the synthesized 30Kc19-HSA nanoparticles were measured using ELS spectrophotometry. Nanoparticle sizes increased with increasing wt. % of the 30Kc19 protein, from 230 nm with 0 wt. % 30Kc19 to 310 nm with 70% wt. % 30Kc19. Polydispersity of the nanoparticles was about 0.1 regardless of the percentage of 30Kc19, indicating uniformly sized nanoparticles (Fig. 7.1A). The zeta

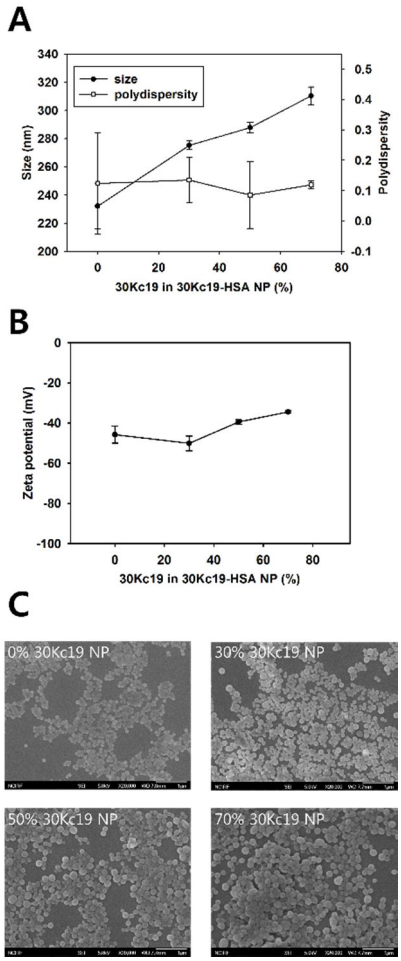


**Figure 7.1** Characterization of the prepared 30Kc19-human serum albumin (HSA) nanoparticles. (A) Nanoparticle size and polydispersity vs. weight percentage (wt. %) of the 30Kc19 protein in the nanoparticles. (B) Zeta potential of nanoparticles. (C) Scanning electron microscopic images of 30Kc19-HSA nanoparticles containing 0–70% wt. % of the 30Kc19 protein (magnification, x 20,000).

potential of the 30Kc19-HSA nanoparticles was ~ −40 mV at neutral pH (Fig. 7.1B), corresponding with stable dispersion of the nanoparticles in water, PBS, and cell culture media. SEM images were obtained to evaluate the effect of the 30Kc19 protein on nanoparticle morphology (Fig. 7.1C). Uniform spherical shapes were observed in all wt. % of the 30Kc19 nanoparticles.

The loading efficiency of α-galactosidase was assessed indirectly using the fluorescently labeled enzyme remaining in the supernatant of the reaction solution (Fig. 7.2A). The α-galactosidase loaded on the nanoparticles with a high yield of 80–95%. Enzyme loading increased slightly with wt. % of 30Kc19 in the nanoparticles.

Enzyme activity of the nanoparticles containing α-galactosidase was measured using a colorimetric assay (Fig. 7.2B). The specific activity of α-galactosidase inside the nanoparticles increased slightly with wt. % of the 30Kc19 protein. Ethanol and glutaraldehyde can damage nanoparticle cargo during preparation. As observed previously, the recombinant 30Kc19 protein stabilizes enzyme activities [8], and the 30Kc19-HSA protein nanoparticles also stabilized cargo activity during the nanocarrier preparation process and after intracellular delivery. As the enzyme stabilizing activity of the nanoparticles is due to the 30Kc19 protein, a higher stabilizing effect of the nanoparticles was observed by increasing the percentage of 30Kc19 in the nanoparticles. However, α-galactosidase activity decreased in 70% wt. % 30Kc19 nanoparticles. This decrease was due to structural instability of the nanoparticles with a high wt. % of the 30Kc19 level.

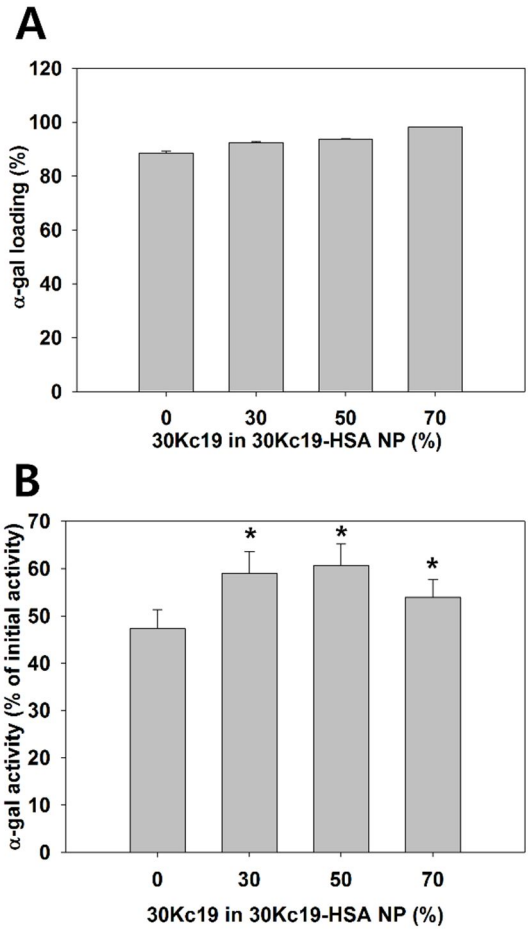


**Figure 7.2** Effect of the 30Kc19 protein on enzyme loading efficiency and enzyme stabilization. (A) α-galactosidase loading efficiency of the 30Kc19-HSA nanoparticles with increasing wt. % (0–70%) of the 30Kc19 protein, which was indirectly measured using the fluorescent-labeled enzyme remaining in the reaction solution supernatant. (B) Activity of α-galactosidase loaded in 30Kc19-human serum albumin (HSA) nanoparticles, as measured by an α-galactosidase activity assay (*$p < 0.05$).

## 7.3 Cellular toxicity of 30Kc19-HSA nanoparticles

Cellular toxicity of the 30Kc19-HSA nanoparticles containing α-galactosidase was measured by the MTT assay (Fig. 7.3). Human foreskin fibroblasts were chosen as the target delivery cell, as a α-galactosidase target would be human primary cells. No significant decrease in MTT reduction was observed in human foreskin fibroblasts in 0–70% wt. % 30Kc19 nanoparticles. HSA and the 30Kc19 protein are reported to be non-toxic *in vitro* and *in vivo* [128], and 30Kc19-HSA nanoparticles show negligible toxicity in HeLa and HEK293 cells [124]. Treatment with the 30Kc19-HSA nanoparticles also resulted in no toxicity to human primary cells, suggesting that using 30Kc19-HSA nanoparticles for drug delivery is acceptable for *in vivo* ERT.

## 7.4 Cellular uptake of nanoparticles

Cellular uptake of the 30Kc19-HSA nanoparticles containing α-galactosidase was assessed using fluorescent-labeled nanoparticles (Fig. 7.4A). 30Kc19-HSA nanoparticles exhibited higher cellular uptake into human foreskin fibroblasts compared with that of HSA nanoparticles. Fibroblasts treated with 30% and 50% wt. % 30Kc19-HSA nanoparticles for 24 h exhibited 1.5-fold higher fluorescence than that of HSA nanoparticle-treated cells, suggesting enhanced cellular uptake due to the cell-penetrating ability of the 30Kc19 protein. Nanoparticles with 70% wt. % 30Kc19 protein showed slightly higher cellular

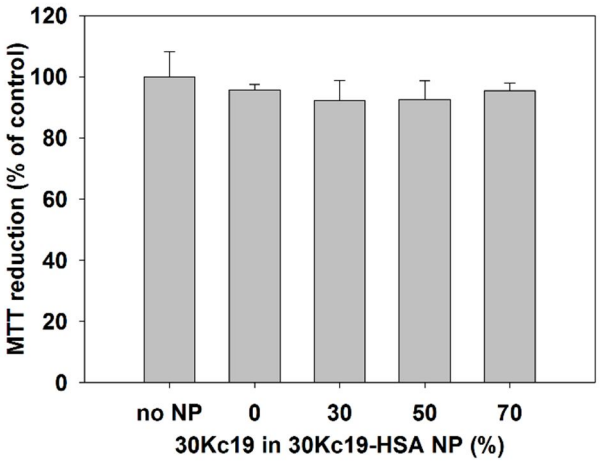


**Figure 7.3** MTT assay of human foreskin fibroblasts treated with 200 μg/ml of the 30Kc19- human serum albumin (HSA) nanoparticles containing 0–50 wt. % of the 30Kc19 protein for 24 h.

uptake than that of HSA nanoparticles, indicating that 30Kc19-HSA nanoparticles have an optimum 30Kc19 proportion for maximum cellular uptake and an enzyme stabilizing effect. This optimum proportion is due to the structural instability of the nanoparticles with a high percentage of 30Kc19.

Confocal microscopic images of human fibroblasts treated with the nanoparticles were taken to assess nanoparticle uptake. After a 24 h treatment, higher fluorescence was observed in cells treated with nanoparticles containing the 30Kc19 protein than that of those with the HSA only nanoparticles (Fig. 7.4B). HSA and 30Kc19-HSA nanoparticle fluorescence was in a punctuate form in the cytoplasmic area, suggesting that the nanoparticles were trapped in late endosomes and lysosomes. Nanoparticles with 50% wt. % 30Kc19 were treated with LysoTracker to verify lysosomal localization of the nanoparticles (Fig. 7.4C). The green fluorescence from the nanoparticles and the red fluorescence from LysoTracker were merged and co-localized as yellow dots, showing the 30Kc19-HSA nanoparticles localized in lysosomes. As α-galactosidase is a drug for lysosomal storage disorders, lysosomal trafficking of 30Kc19-HSA nanoparticles could be suitable for cellular α-galactosidase delivery.

## 7.5 Intracellular α-galactosidase activity delivered by nanoparticles

To investigate the activity of α-galactosidase delivered directly or via the protein nanoparticles, human foreskin fibroblasts were treated with α-

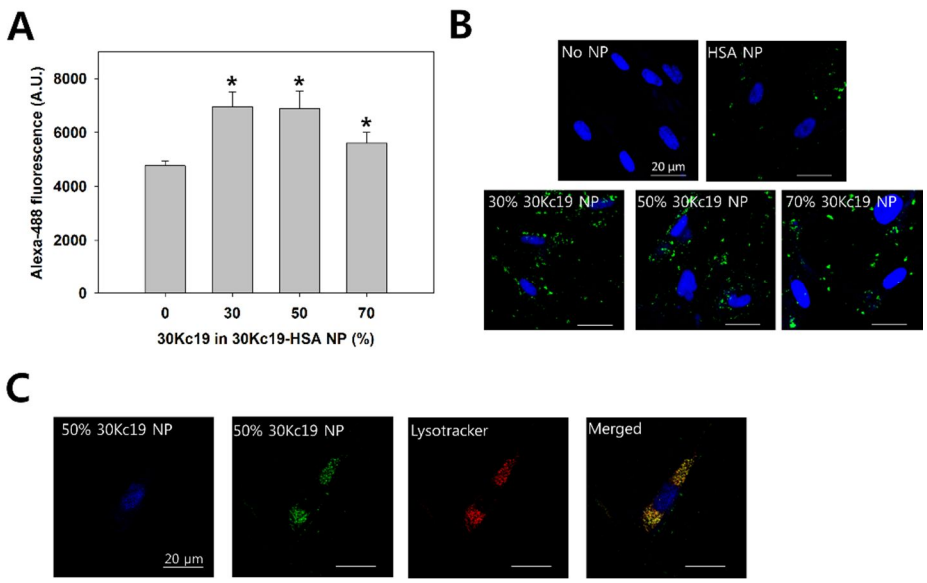


**Figure 7.4** Cellular uptake of 30Kc19-human serum albumin (HSA) nanoparticles. (A) Quantitative cellular uptake of 30Kc19-HSA nanoparticles containing 0–70 wt. % of the 30Kc19 protein, as measured using Alexa Fluor® 488-labeled nanoparticles. Human foreskin fibroblasts were treated with the nanoparticles for 24 h, and fluorescence was measured using a fluorometer. (B) Confocal microscopic image of human foreskin fibroblasts treated with 200 μg/ml of 30Kc19-HSA nanoparticles containing 0–70 wt.% of the 30Kc19 protein for 24 h. The nanoparticles were labeled with Alexa-Fluor® 488 (green fluorescence), and nuclei were stained with Hoechst 33342 (blue fluorescence). (C) Lysosomal targeting of 50% wt.% 30Kc19-HSA nanoparticles in human foreskin fibroblasts. Nanoparticles were labeled with Alexa-Fluor® 488 (green fluorescence), and lysosomes were labeled with Lysotracker (red fluorescence).

galactosidase, α-galactosidase-containing HSA nanoparticles, or α-galactosidase-containing 30Kc19-HSA nanoparticles for 24 h, and α-galactosidase activity of the cell lysates was assayed using a colorimetric method (Fig. 7.5). Cells treated with α-galactosidase and α-galactosidase-containing HSA nanoparticles exhibited very limited intracellular α-galactosidase activity after 24 h, suggesting rapid deactivation of α-galactosidase delivered to cells. However, α-galactosidase delivered using the 30Kc19-HSA nanoparticles retained enzyme activity after 24 h, and 50% wt. % 30Kc19-HSA nanoparticles exhibited the highest α-galactosidase activity. As shown in Fig. 4A, 30% and 50% wt. % 30Kc19-HSA nanoparticles had higher cellular uptake; however, 70% wt. % 30Kc19-HSA nanoparticles showed relatively higher α-galactosidase activity than that of 30% wt. % 30Kc19-HSA nanoparticles. This result indicates that 30Kc19 plays a role for the cargo enzyme stability not only during the preparation of nanoparticles but also in nanoparticles after cellular uptake [124]. The 30Kc19 protein exhibited enhanced cargo stability, which is crucial for contemporary *in vivo* drug delivery. Furthermore, the enhancement of α-galactosidase activity was highest in nanoparticles with 50% wt. % 30Kc19, indicating the optimal 30Kc19 percentage in nanoparticles.

## 7.6 Globotriaosylceramide degradation activity in nanoparticle-treated Fabry disease fibroblasts

The therapeutic efficiency of 30Kc19-HSA nanoparticles containing α-

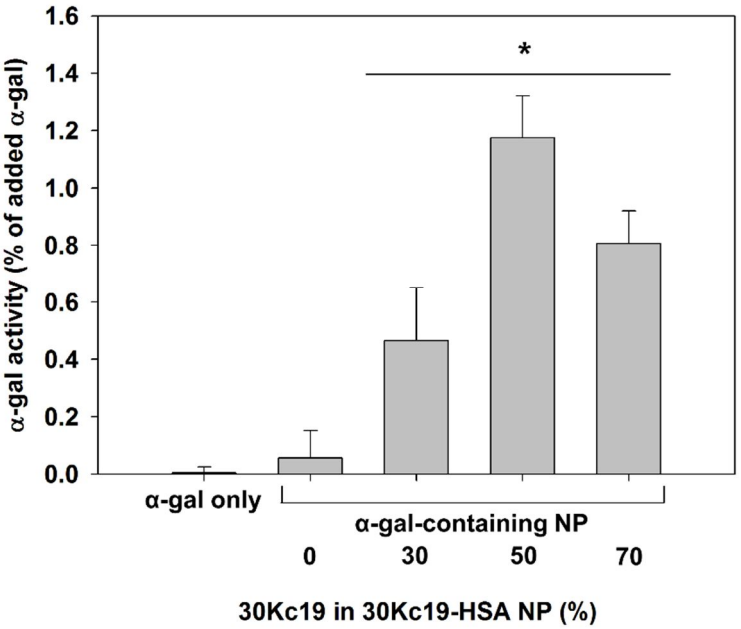


**Figure 7.5** Quantitative analysis of α-galactosidase activity in human foreskin fibroblasts treated with 30Kc19-human serum albumin (HSA) nanoparticles containing α-galactosidase and 0–70 wt. % of the 30Kc19 protein. α-Galactosidase was added to the media at 4 μg/ml. Intracellular α-galactosidase activity was measured after a 24 h incubation (*$p < 0.05$).

galactosidase was assessed using fibroblasts from a patient with Fabry disease. Fabry fibroblasts were pre-treated with the Gb3 fluorescent analog, and α-galactosidase, α-galactosidase-containing HSA nanoparticles, and α-galactosidase-containing 50% wt. % 30Kc19-HSA nanoparticles was added. Then, Gb3 degradation activity was visualized (Fig. 7.6A) and quantified using a fluorometer (Fig. 7.6B). After 24 h, 29% of the initial NBD-GB3 was degraded in the α-galactosidase-treated cells, whereas α-galactosidase-containing HSA nanoparticles exhibited only 12% NBD-GB3 degradation. As α-galactosidase can be internalized into cells and targeted to lysosomes via the mannose 6-phosphate receptor, α-galactosidase has high uptake efficiency into cells and lysosomal targeting. Although HSA has its own receptor-mediated endocytosis pathway, α-galactosidase showed higher cellular uptake activity than that of the HSA nanoparticles because of size. The 50% wt. % 30Kc19-HSA nanoparticles degraded 47% of the NBD-GB3, which was 3.8-fold higher than that of the HSA nanoparticles and 1.6-fold higher than that of α-galactosidase itself. Considering the 1.5-fold enhancement in cellular uptake of 30Kc19-HSA nanoparticles over HSA nanoparticles, the enhanced NBD-GB3 degradation could be mainly due to a cargo stabilizing effect of the 30Kc19 protein in the nanoparticles. This stabilization effect would be even more effective when applied *in vivo* because of degradation by proteases and the immune reaction.

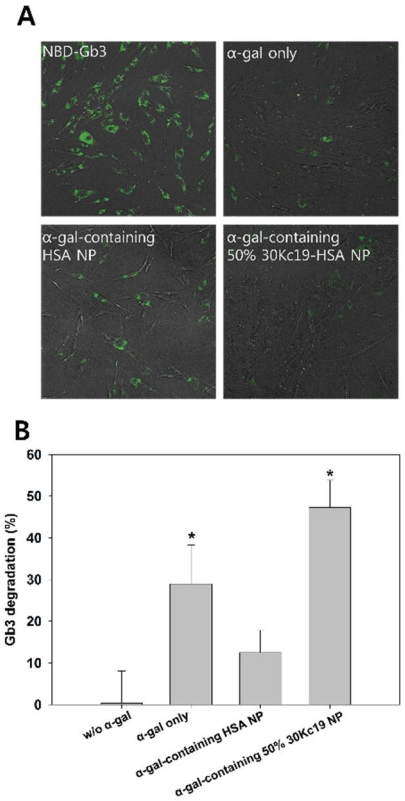


**Figure 7.6** Globotriaosylceramide degradation activity in nanoparticle-treated Fabry disease fibroblasts. Fibroblasts from a patient with Fabry disease (pre-treated with NBD-GB3) were treated with α-galactosidase, α-galactosidase-containing human serum albumin (HSA) nanoparticles, or α-galactosidase-containing 50% wt. % 30Kc19 nanoparticles for 24 h. α-Galactosidase was added to the media at 4 μg/ml. (A) Fluorescence microscopy image of the Fabry fibroblasts treated with α-galactosidase only, α-galactosidase-containing HSA nanoparticles, or α-galactosidase-containing 50% wt. % 30Kc19 nanoparticles. Green fluorescence represents remaining NBD-GB3. (B) Quantitative analysis of Gb3 degradation using a fluorometer.

## 7.7 Conclusions

The 30Kc19 protein, which has cell-penetrating and protein-stabilizing properties, was used with HSA to synthesize protein nanoparticles loaded with α-galactosidase to treat Fabry disease. The α-galactosidase-containing 30Kc19-HSA nanoparticles were spherical in shape, uniform in size, and had high loading efficiency for α-galactosidase. The 30Kc19 stabilized α-galactosidase during nanoparticle preparation. The 30Kc19-HSA nanoparticles also exhibited enhanced uptake into human foreskin fibroblasts and higher α-galactosidase activity than that of HSA nanoparticles. The α-galactosidase-containing 30Kc19-HSA protein nanoparticles were targeted to lysosomes and showed enhanced Gb3 degradation over α-galactosidase-containing HSA nanoparticles or α-galactosidase itself in fibroblasts from a patient with Fabry disease. These 30Kc19-HSA nanoparticles are expected to be used as effective nanocarrier for ERT in patients with Fabry disease. Furthermore, these nanoparticles are a versatile tool for intracellular delivery of therapeutic proteins, and a specific anti-cancer drug delivery vehicle when combined with cell targeting ligands.

# Chapter 8.

# Overall discussion and further suggestions

# Chapter 8. Overall discussion and further suggestions

## 8.1 Overall discussion

In a previous study, an increase in the mitochondrial membrane potential was observed with the expression of 30Kc19 in CHO cells [6]. These simultaneous effects resulted in improved productivity of a therapeutic protein. However, it was not clearly understood how the 30Kc19 enhanced these intracellular biological processes. Recently, it was demonstrated that 30Kc19 has a stabilizing effect on various enzymes, apparently non-specifically [8]. Based on these previous results, it was hypothesized that 30Kc19 stabilized the intracellular enzymes involved in the mitochondrial electron transfer process *in vitro*. The effects of 30Kc19 on intracellular mitochondrial activities through supplementation of recombinant 30Kc19 into the culture medium was also investigated.

In the quantitative analysis of *in vitro* mitochondrial enzyme complex activity, the 30Kc19-treated group showed no difference in effect when compared with the control at the early stage. However, in the presence of 30Kc19, the rate was maintained throughout the course, even at the late stage, while the reaction rate decreased rapidly as time passed in the absence of 30Kc19. In initial phase, deactivation of mitochondrial complex enzyme is negligible and stabilizing effect of 30Kc19 is not visible. However, environmental deactivation of mitochondrial complex enzyme is noticeable as reaction progresses to the late phase and thus stabilizing effect of 30Kc19 is clearly observed. These results

suggested that the stability of the mitochondrial complex enzyme was improved by 30Kc19, even though mitochondrial complex enzyme still gradually lost activity because of its low stability. Hence, kinetic stability of mitochondrial complex enzyme was enhanced by 30Kc19 from environmental deactivation in long-term operation. It is noticeable that time kinetics of 30Kc19-treated group is still a first order reaction. It is suggested that 30Kc19 seems to have non-specific stabilizing activity rather than specific activity. Based on these findings, it was conclude that 30Kc19 improves the stability of enzymes involved in mitochondrial electron transport. While 30Kc19 stabilized mitochondrial complex activity, a high concentration of 30Kc19 was needed to stabilize intracellular mitochondrial enzyme complex (200 - 1000 μg/ml). It has been reported that mitochondrial signal sequence protein fused with TAT protein exhibited enhanced mitochondrial uptake and retention over TAT protein in GFP protein delivery [133]. That is, because 30Kc19 lacks a mitochondrial signal sequence, it has less accessibility to mitochondria despite its cell-penetrating ability. Thus, a high concentration of 30Kc19 was needed for the mitochondrial complex because of the mitochondrial accessibility of 30Kc19.

Subsequently, when recombinant 30Kc19 was added to cell culture medium, increases in the activities of mitochondrial complex were observed, improving the ATP generation from mitochondria. The 30Kc19 has the ability to penetrate into cells and mitochondria [124], and it can enhance the stability of cellular mitochondrial complex, as it does *in vitro* experiments, leading to enhanced glycosylation and ATP production. The results described here explain how

recombinant protein productivity and glycosylation were enhanced by the expression of 30Kc19, or the addition of recombinant 30Kc19, which were proposed in previous studies [6, 7]. According to this report, it is supposed that the improvements in productivity in mammalian cells are due to stabilizing effects of 30Kc19 on mitochondrial enzymes. It is known that recombinant protein production can be affected by such stresses as nutrient depletion, hypoxia, shear stress, and accumulation of toxic byproducts, all of which occur frequently during industrial mammalian cell culture for the production of recombinant proteins [134-136]. Mitochondrial enzymes are damaged by those factors, resulting in reduced mitochondrial oxidative capacity [137]. Decreased mitochondrial respiration results in the disruption of mitochondrial membrane potential and loss of ATP generation, which is associated with low productivity. According to a previous study showing that 30Kc19 stabilized various enzymes *in vitro* [8], the stabilizing effect is believed to be due to a direct interaction between 30Kc19 and the enzymes. Further investigation is required to understand the exact mechanism at the molecular level.

It is crucial for a drug delivery vehicle to have enhanced uptake efficiency and prolonged activity *in vivo*. Although the desolvation method is widely used to prepare protein nanoparticles because it is a simple and fast preparation process, the ethanol and glutaraldehyde used in the preparation process could damage the nanoparticle cargo, particularly therapeutic proteins [120]. In this study, the recombinant 30Kc19 protein was applied to HSA nanoparticles to stabilize the therapeutic protein cargo. The previous report showed that the recombinant

30Kc19 protein stabilizes conventionally known enzymes under both moderate and harsh conditions *in vitro* [8]. It was also reported that recombinant human erythropoietin production and sialylation in CHO cells were enhanced by 30Kc19 gene expression in the cells, based on stabilization of sialyl transferase activity and the mitochondrial enzyme complex in CHO cells [7]. In previous studies, it was suggested that the enzyme stabilizing activity of the 30Kc19 protein is due to a shielding effect rather than a specific molecule-molecule interaction with enzymes, as 30Kc19 has a stabilizing effect on various enzymes only when at a much higher concentration (200–15,000 fold) than the enzyme. Further investigations are required to elucidate the precise stabilization mechanism of the enzyme by the 30Kc19 protein. Based on these studies, applying the 30Kc19 protein to HSA nanoparticles was expected to stabilize activity of the enzyme cargo not only during the preparation process but also in the intracellular environment after delivery to the cells. β-Galactosidase activity remaining in the supernatant, released *in vitro*, and delivered into cells was measured for verification. All experiments successfully demonstrated that the 30Kc19 protein stabilized the β-galactosidase activity at all stages from preparation of the nanocarrier to intracellular delivery. In particular, despite only a slight increase in cellular uptake over HSA nanoparticles were shown, 50% 30Kc19-HSA nanoparticles exhibited a much higher β-galactosidase activity than nanoparticles without 30Kc19 in HeLa cells. It suggests that enhanced β-galactosidase activity is due to not only enhanced cellular uptake but also enzyme-stabilizing activity of 30Kc19 protein.

It was interesting that the 30Kc19-HSA nanoparticles exhibited optimal enzyme cargo activity and *in vitro* release. As observed in the SEM images, the 30Kc19-HSA nanoparticles with higher 30Kc19 content had a less-packed matrix structure. This might be the cause for the increase in the *in vitro* release of the 30Kc19-HSA nanoparticles with up to 50 wt.% 30Kc19 protein compared with HSA-only protein nanoparticles. The nanoparticle matrix was so disrupted in the case of nanoparticles with > 70 wt.% 30Kc19 protein that ethanol and glutaraldehyde could invade not only the surface but also the inner matrix of the nanoparticles, leading to decreased enzyme cargo activity and *in vitro* release due to crosslinking between the enzyme cargo and protein matrix inside the nanoparticles.

Because the 30Kc19 protein exhibits cell-penetrating properties and can deliver cargo proteins into cells *in vitro* and tissues *in vivo* [124], intracellular uptake of the protein nanoparticles was assessed using confocal laser scanning microscopy and flow cytometry to determine whether the 30Kc19 protein enhanced uptake efficiency into cells in the form of protein nanoparticles. Cellular uptake of nanoparticles typically occurs by diverse endocytosis routes. Nanoparticles up to 200 nm in diameter are internalized mainly via clathrin-mediated endocytosis, whereas nanoparticles larger than 200 nm are internalized via multiple endocytotic pathways, such as caveolae-mediated endocytosis and macropinocytosis. [138]. Although HEK293 cells have limited caveolae-mediated endocytosis, they seem to have more active endocytotic routes for 30Kc19-HSA nanoparticles than HeLa cells. Thus, difference in

cellular uptake may originate from different endocytotic efficiency of the two cell lines. The effect of the 30Kc19 protein on nanoparticle uptake efficiency varied between the two cell lines. HeLa cells have the gp60 albumin-binding receptor located at the caveolae on cell membranes. Thus, HSA and HSA nanoparticles penetrate into cells upon binding to the receptor [139]. Therefore, the decreased amount of HSA in 30Kc19-HSA nanoparticles compared with pure HSA nanoparticles indicates a decrease in 30Kc19-HSA nanoparticle internalization by gp60-mediated endocytosis in HeLa cells. Nevertheless, the cell-penetrating property of the 30Kc19 protein compensated or rather increased cellular delivery of the 30Kc19-HSA nanoparticles. This explanation was clearly demonstrated in the results using HEK293 cells, which have very few caveolae [140, 141]. The delivery effect of the 30Kc19-HSA nanoparticles compared with HSA nanoparticles was more obvious.

Human foreskin fibroblasts were chosen as the target delivery cell for observation of cellular uptake and intracellular α-galactosidase activity, as a α-galactosidase target would be human primary cells. The 30Kc19 protein exhibited enhanced cargo stability, which is crucial for contemporary *in vivo* drug delivery. Furthermore, the optimum 30Kc19 percentage in nanoparticles for the intracellular α-galactosidase activity, potentially caused by structural instability of the nanoparticles with a high wt. % of the 30Kc19 level, also was observed (Fig. 7.5).

The 30Kc19-HSA nanoparticles containing α-galactosidase was treated to Fabry disease fibroblasts to investigate therapeutic efficiency (Fig. 7.6). As α-

galactosidase can be internalized into cells and targeted to lysosomes via the mannose 6-phosphate receptor, α-galactosidase has high uptake efficiency into cells and lysosomal targeting. Although HSA has its own receptor-mediated endocytosis pathway, α-galactosidase showed higher cellular uptake activity than that of the HSA nanoparticles because of size. Considering the 1.5-fold enhancement in cellular uptake of 30Kc19-HSA nanoparticles over HSA nanoparticles, the enhanced NBD-GB3 degradation could be mainly due to a cargo stabilizing effect of the 30Kc19 protein in the nanoparticles. This stabilization effect would be even more effective when applied *in vivo* because of degradation by proteases and the immune reaction.

## 8.2 Conclusion and further suggestions

Firstly, *in vitro* stabilization of the mitochondrial enzyme complex by 30Kc19, which are related to protein productivity in industrial mammalian cell culture was observed. Furthermore, intracellular enzyme stability was increased by adding 30Kc19 to the culture medium.

With these results, using 30Kc19 as building block of protein nanoparticles was attempted. The protein nanoparticles using 30Kc19 protein were produced and characterized by using hybridization with HSA to secure stability of nanoparticle structure. 30Kc19-HSA nanoparticles were prepared with uniform spherical morphology and stable dispersion in buffer and culture media. 30Kc19-HSA nanoparticles showed negligible toxicity when treated to HeLa cells, and showed enhanced uptake to cells with little caveolae, limiting uptake

of HSA-based nanoparticles exploiting caveolae-mediated endocytosis.

Because 30Kc19-HSA nanoparticles exhibit enhanced cellular uptake, the model protein cargo was loaded to them to investigate whether 30Kc19 in nanoparticles stabilize protein cargo. β-Galactosidase was loaded to 30Kc19-HSA nanoparticles simultaneously with nanoparticle formation. 30Kc19-HSA nanoparticles loaded efficiently β-galactosidase, and stable structure and dispersion was observed. Sustained release of β-Galactosidase was observed in 30Kc19-HSA nanoparticles, and released enzyme was more stabilized in 30Kc19-HSA nanoparticles compared with HSA nanoparticles. The 30Kc19-HSA nanoparticles enhanced cellular uptake, particularly in cells with limited caveolae, and β-galactosidase activity when compared with the HSA nanoparticles.

Since 30Kc19-HSA nanoparticles proved to be efficient nanocarrier to enhance both cellular uptake and stability of enzyme cargo, 30Kc19-HSA protein nanoparticles were loaded with α-galactosidase, therapeutics for Fabry disease and its possibility as drug carrier was investigated. The α-galactosidase-containing 30Kc19-HSA nanoparticles was successfully synthesized in spherical shape and uniform size. 30Kc19-HSA nanoparticles showed high loading efficiency for α-galactosidase, and also exhibited enhanced cellular uptake and higher α-galactosidase activity in human foreskin fibroblasts, compared with HSA nanoparticles. Finally, the α-galactosidase-containing 30Kc19-HSA protein nanoparticles were targeted to lysosomes and exhibited enhanced Gb3 degradation compared with HSA nanoparticles or α-

galactosidase itself in Fabry patient fibroblasts.

Thus, 30Kc19-HSA nanoparticles are promising nanocarrier for intracellular delivery of therapeutic proteins with enhanced uptake and stability. Furthermore, 30Kc19-HSA nanoparticles would be specific anti-cancer drug delivery vehicle if combined with appropriate cell targeting ligands, such as peptide or antibodies.

The 30Kc19 protein has two domains; an N-terminal domain consisting of α-helices and a C-terminal domain consisting of β-sheets [31]. In study, it seemed that the 30Kc19 protein has a short peptide domain located at the N-terminal domain that was responsible for the cell-penetrating effect. If the N-terminal domain has a cell-penetrating ability, in was hypothesized that the C-terminal domain is responsible for the enzyme-stabilizing property of the 30Kc19 protein. It is currently investigated the activity of each 30Kc19 domain through 30Kc19 truncation and an activity assessment of the 30Kc19 truncated domains.

The 30Kc19 protein in the 30Kc19-HSA nanoparticles had cell-penetrating and protein-stabilizing activities. However, the percentage of 30Kc19 in nanoparticles was limited because of structural instability caused by increasing 30Kc19 content in the nanoparticles. If nanoparticles can be stably formed using only the 30Kc19 protein, the beneficial effect of the 30Kc19 protein on cargo uptake and stabilization could be maximized. The 30Kc19 protein consists of an N-terminal domain α-helices and C-terminal domain β-sheets [142]. According to the study, the 30Kc19 protein has a short cell-penetrating peptide at the N-terminal domain [143]. Recombinant N-terminal domain α-

helices of the 30Kc19 protein was produced, and observed that it exhibits similar protein-stabilizing activity. Further study is required to investigate whether the protein nanoparticles can be stably formed using the N-terminal domain α-helices of 30Kc19.

## References


[1] Rhee WJ, Kim EJ, Park TH. Kinetic Effect of Silkworm Hemolymph on the Delayed Host Cell Death in an Insect Cell-Baculovirus System. Biotechnology Progress. 1999;15(6):1028-32.

[2] Rhee WJ, Park TH. Silkworm hemolymph inhibits baculovirus-induced insect cell apoptosis. Biochemical and Biophysical Research Communications. 2000;271(1):186-90.

[3] Kim EJ, Park HJ, Park TH. Inhibition of apoptosis by recombinant 30K protein originating from silkworm hemolymph. Biochemical and Biophysical Research Communications. 2003;308(3):523-8.

[4] Choi SS, Rhee WJ, Park TH. Beneficial effect of silkworm hemolymph on a CHO cell system: Inhibition of apoptosis and increase of EPO production. Biotechnology and Bioengineering. 2005;91(7):793-800.

[5] Choi SS, Rhee WJ, Kim EJ, Park TH. Enhancement of recombinant protein production in Chinese hamster ovary cells through anti-apoptosis engineering using *30Kc6* gene. Biotechnology and Bioengineering. 2006;95(3):459-67.

[6] Wang Z, Park JH, Park HH, Tan W, Park TH. Enhancement of recombinant human EPO production and sialylation in Chinese hamster ovary cells through *Bombyx mori 30Kc19* gene expression. Biotechnology and Bioengineering. 2011;108(7):1634-42.

[7] Park JH, Wang Z, Jeong H-J, Park HH, Kim B-G, Tan W-S, Choi SS, Park TH. Enhancement of recombinant human EPO production and glycosylation in serum-free suspension culture of CHO cells through expression and supplementation of 30Kc19. Applied Microbiology and Biotechnology. 2012;96(3):671-83.

[8] Park JH, Park HH, Choi SS, Park TH. Stabilization of enzymes by the recombinant 30Kc19 protein. Process Biochemistry. 2012;47(1):164-9.

[9] Fágáin CÓ. Understanding and increasing protein stability. Biochimica et Biophysica Acta (BBA)-Protein Structure and Molecular Enzymology. 1995;1252(1):1-14.

[10] Jakobsson P-J, Thorén S, Morgenstern R, Samuelsson B. Identification of human prostaglandin E synthase: a microsomal, glutathione-dependent, inducible enzyme, constituting a potential novel drug target. Proceedings of the National Academy of Sciences. 1999;96(13):7220-5.

[11] Hurley LH. DNA and associated targets for drug design. Journal of Medicinal Chemistry. 1989;32(9):2027-33.

[12] Rubino OP, Kowalsky R, Swarbrick J. Albumin microspheres as a drug delivery system: relation among turbidity ratio, degree of cross-linking, and drug release. Pharmaceutical Research. 1993;10(7):1059-65.

[13] Kommareddy S, Amiji M. Preparation and evaluation of thiol-modified gelatin nanoparticles for intracellular DNA delivery in response to glutathione. Bioconjugate Chemistry. 2005;16(6):1423-32.

[14] Azarmi S, Tao X, Chen H, Wang Z, Finlay WH, Löbenberg R, Roa WH. Formulation and cytotoxicity of doxorubicin nanoparticles carried by dry powder aerosol particles. International Journal of Pharmaceutics. 2006;319(1):155-61.

[15] Macan P. Definitions of Terms Relating to the Structure and Processing of Sols, Gels, Networks, and Inorganic-Organic Hybrid Materials. Kemija u industriji. 2011;60(3):135-53.

[16] Vert M, Hellwich K-H, Hess M, Hodge P, Kubisa P, Rinaudo M, Schué F. Terminology for biorelated polymers and applications (IUPAC Recommendations 2012). Pure and Applied Chemistry. 2012;84(2):377-410.

[17] Madani SY, Naderi N, Dissanayake O, Tan A, Seifalian AM. A new era of cancer treatment: carbon nanotubes as drug delivery tools. International journal of nanomedicine. 2011;6):2963.

[18] Gao J, Gu H, Xu B. Multifunctional magnetic nanoparticles: design, synthesis, and biomedical applications. Accounts of Chemical Research. 2009;42(8):1097-107.

[19] Fan Z, Shelton M, Singh AK, Senapati D, Khan SA, Ray PC. Multifunctional plasmonic shell–magnetic core nanoparticles for targeted diagnostics, isolation, and photothermal destruction of tumor cells. ACS nano. 2012;6(2):1065-73.

[20] Hao R, Xing R, Xu Z, Hou Y, Gao S, Sun S. Synthesis, functionalization, and biomedical applications of multifunctional magnetic nanoparticles. Advanced Materials. 2010;22(25):2729-42.

[21] Kim JA, Lee HJ, Kang H-J, Park TH. The targeting of endothelial progenitor cells to a specific location within a microfluidic channel using magnetic nanoparticles. Biomedical Microdevices. 2009;11(1):287-96.

[22] Song JW, Gu W, Futai N, Warner KA, Nor JE, Takayama S. Computer-controlled microcirculatory support system for endothelial cell culture and shearing. Analytical Chemistry. 2005;77(13):3993-9.

[23] Mai WX, Meng H. Mesoporous silica nanoparticles: A multifunctional nano therapeutic system. Integrative Biology. 2013;5(1):19-28.

[24] Benezra M, Penate-Medina O, Zanzonico PB, Schaer D, Ow H, Burns A, DeStanchina E, Longo V, Herz E, Iyer S. Multimodal silica nanoparticles are effective cancer-targeted probes in a model of human melanoma. The Journal of clinical investigation. 2011;121(7):2768-80.

[25] Trewyn BG, Slowing II, Giri S, Chen H-T, Lin VS-Y. Synthesis and functionalization of a mesoporous silica nanoparticle based on the sol–gel process and applications in controlled release. Accounts of Chemical Research. 2007;40(9):846-53.

[26] Minati L, Antonini V, Dalla Serra M, Speranza G. Multifunctional branched gold–carbon nanotube hybrid for cell imaging and drug delivery. Langmuir. 2012;28(45):15900-6.

[27] Chen T, Xu S, Zhao T, Zhu L, Wei D, Li Y, Zhang H, Zhao C. Gold nanocluster-conjugated amphiphilic block copolymer for tumor-targeted drug delivery. ACS applied materials & interfaces. 2012;4(11):5766-74.

[28] Zhang Z, Wang L, Wang J, Jiang X, Li X, Hu Z, Ji Y, Wu X, Chen C. Mesoporous Silica-Coated Gold Nanorods as a Light-Mediated Multifunctional Theranostic Platform for Cancer Treatment. Advanced Materials. 2012;24(11):1418-23.

[29] Hoskins C, Min Y, Gueorguieva M, McDougall C, Volovick A, Prentice P, Wang Z, Melzer A, Cuschieri A, Wang L. Hybrid gold-iron oxide nanoparticles as a multifunctional platform for biomedical application. J Nanobiotechnol. 2012;10):27.

[30] Petersen LK, Ramer-Tait AE, Broderick SR, Kong C-S, Ulery BD, Rajan K, Wannemuehler MJ, Narasimhan B. Activation of innate immune responses in a pathogen-mimicking manner by amphiphilic polyanhydride nanoparticle adjuvants. Biomaterials. 2011;32(28):6815-22.

[31] Zrazhevskiy P, Sena M, Gao X. Designing multifunctional quantum dots for bioimaging, detection, and drug delivery. Chemical Society Reviews. 2010;39(11):4326-54.

[32] Biju V, Itoh T, Ishikawa M. Delivering quantum dots to cells:

bioconjugated quantum dots for targeted and nonspecific extracellular and intracellular imaging. Chemical Society Reviews. 2010;39(8):3031-56.

[33] Lukyanov AN, Torchilin VP. Micelles from lipid derivatives of water-soluble polymers as delivery systems for poorly soluble drugs. Advanced Drug Delivery Reviews. 2004;56(9):1273-89.

[34] Blanco E, Kessinger CW, Sumer BD, Gao J. Multifunctional micellar nanomedicine for cancer therapy. Experimental Biology and Medicine. 2009;234(2):123-31.

[35] Hu Y-Y, Liu X, Ma X, Rawal A, Prozorov T, Akinc M, Mallapragada S, Schmidt-Rohr K. Biomimetic self-assembling copolymer−hydroxyapatite nanocomposites with the nanocrystal size controlled by citrate. Chemistry of Materials. 2011;23(9):2481-90.

[36] Jia F, Zhang Y, Narasimhan B, Mallapragada SK. Block copolymer-quantum dot micelles for multienzyme colocalization. Langmuir. 2012;28(50):17389-95.

[37] Luppi B, Bigucci F, Cerchiara T, Andrisano V, Pucci V, Mandrioli R, Zecchi V. Micelles based on polyvinyl alcohol substituted with oleic acid for targeting of lipophilic drugs. Drug Delivery. 2004;12(1):21-6.

[38] Torchilin VP. Micellar nanocarriers: pharmaceutical perspectives. Pharmaceutical Research. 2007;24(1):1-16.

[39] Fares MM, Assaf SM, Jaber AA. Biodegradable amphiphiles of grafted poly (lactide) onto 2-hydroxyethyl methacrylate-co-N-vinylpyrrolidone copolymers as drug carriers. Journal of Applied Polymer Science. 2011;122(2):840-8.

[40] Batrakova EV, Vinogradov SV, Robinson SM, Niehoff ML, Banks WA, Kabanov AV. Polypeptide point modifications with fatty acid and amphiphilic block copolymers for enhanced brain delivery. Bioconjugate Chemistry. 2005;16(4):793-802.

[41] Andresen TL, Thompson DH, Kaasgaard T. Enzyme-triggered nanomedicine: Drug release strategies in cancer therapy (Invited Review). Molecular Membrane Biology. 2010;27(7):353-63.

[42] Lian T, Ho RJ. Trends and developments in liposome drug delivery systems. Journal of Pharmaceutical Sciences. 2001;90(6):667-80.

[43] Düzgüneş N, Nir S. Mechanisms and kinetics of liposome–cell interactions. Advanced Drug Delivery Reviews. 1999;40(1):3-18.

[44] Al-Jamal WT, Kostarelos K. Liposomes: from a clinically established drug delivery system to a nanoparticle platform for theranostic nanomedicine. Accounts of Chemical Research. 2011;44(10):1094-104.

[45] Chacko RT, Ventura J, Zhuang J, Thayumanavan S. Polymer nanogels: A versatile nanoscopic drug delivery platform. Advanced Drug Delivery Reviews. 2012;64(9):836-51.

[46] Raemdonck K, Demeester J, De Smedt S. Advanced nanogel engineering for drug delivery. Soft Matter. 2009;5(4):707-15.

[47] Morimoto N, Hirano S, Takahashi H, Loethen S, Thompson DH, Akiyoshi K. Self-assembled pH-sensitive cholesteryl pullulan nanogel as a protein delivery vehicle. Biomacromolecules. 2012;14(1):56-63.

[48] Chen Y, Wilbon PA, Zhou J, Nagarkatti M, Wang C, Chu F, Tang C. Multifunctional self-fluorescent polymer nanogels for label-free imaging and drug delivery. Chemical Communications. 2013;49(3):297-9.

[49] Khandare J, Calderón M, Dagia NM, Haag R. Multifunctional dendritic polymers in nanomedicine: opportunities and challenges. Chemical Society Reviews. 2012;41(7):2824-48.

[50] Astruc D, Boisselier E, Ornelas C. Dendrimers designed for functions: from physical, photophysical, and supramolecular properties to applications in sensing, catalysis, molecular electronics, photonics, and nanomedicine. Chemical Reviews. 2010;110(4):1857-959.

[51] Shenoi RA, Narayanannair JK, Hamilton JL, Lai BF, Horte S, Kainthan RK, Varghese JP, Rajeev KG, Manoharan M, Kizhakkedathu JN. Branched multifunctional polyether polyketals: variation of ketal group structure enables unprecedented control over polymer degradation in solution and within cells. Journal of the American Chemical Society. 2012;134(36):14945-57.

[52] Harper BW, Krause-Heuer AM, Grant MP, Manohar M, Garbutcheon-Singh KB, Aldrich-Wright JR. Advances in platinum chemotherapeutics. Chemistry-A European Journal. 2010;16(24):7064-77.

[53] Wang Q, Wang L, Detamore MS, Berkland C. Biodegradable colloidal gels as moldable tissue engineering scaffolds. Advanced Materials. 2008;20(2):236-9.

[54] Liu Z, Jiao Y, Wang Y, Zhou C, Zhang Z. Polysaccharides-based

nanoparticles as drug delivery systems. Advanced Drug Delivery Reviews. 2008;60(15):1650-62.

[55] Kuijpers A, Van Wachem P, Van Luyn M, Brouwer L, Engbers G, Krijgsveld J, Zaat S, Dankert J, Feijen J. *In vitro* and *in vivo* evaluation of gelatin–chondroitin sulphate hydrogels for controlled release of antibacterial proteins. Biomaterials. 2000;21(17):1763-72.

[56] Elzoghby AO, Abo El-Fotoh WS, Elgindy NA. Casein-based formulations as promising controlled release drug delivery systems. Journal of Controlled Release. 2011;153(3):206-16.

[57] Kratz F, Fichtner I, Beyer U, Schumacher P, Roth T, Fiebig H, Unger C. 784-Antitumour activity of acid labile transferrin and albumin doxorubicin conjugates in *in vitro* and *in vivo* human tumour xenograft models. European Journal of Cancer. 1997;33):S175.

[58] Rahimnejad M, Jahanshahi M, Najafpour G. Production of biological nanoparticles from bovine serum albumin for drug delivery. African Journal of Biotechnology. 2010;5(20).

[59] Weber C, Coester C, Kreuter J, Langer K. Desolvation process and surface characterisation of protein nanoparticles. International Journal of Pharmaceutics. 2000;194(1):91-102.

[60] Irache J, Merodio M, Arnedo A, Camapanero M, Mirshahi M, Espuelas S. Albumin nanoparticles for the intravitreal delivery of anticytomegaloviral drugs. Mini Reviews in Medicinal Chemistry. 2005;5(3):293-305.

[61] Jia F, Liu X, Li L, Mallapragada S, Narasimhan B, Wang Q. Multifunctional nanoparticles for targeted delivery of immune activating and cancer therapeutic agents. Journal of Controlled Release. 2013;172(3):1020-34.

[62] Wongsasulak S, Patapeejumruswong M, Weiss J, Supaphol P, Yoovidhya T. Electrospinning of food-grade nanofibers from cellulose acetate and egg albumen blends. Journal of Food Engineering. 2010;98(3):370-6.

[63] Hu Y-J, Liu Y, Sun T-Q, Bai A-M, Lü J-Q, Pi Z-B. Binding of anti-inflammatory drug cromolyn sodium to bovine serum albumin. International Journal of Biological Macromolecules. 2006;39(4):280-5.

[64] Tantra R, Tompkins J, Quincey P. Characterisation of the de-agglomeration effects of bovine serum albumin on nanoparticles in

aqueous suspension. Colloids and Surfaces B: Biointerfaces. 2010;75(1):275-81.

[65] Hirose M, Tachibana A, Tanabe T. Recombinant human serum albumin hydrogel as a novel drug delivery vehicle. Materials Science and Engineering: C. 2010;30(5):664-9.

[66] Kratz F. Albumin as a drug carrier: design of prodrugs, drug conjugates and nanoparticles. Journal of Controlled Release. 2008;132(3):171-83.

[67] Fasano M, Curry S, Terreno E, Galliano M, Fanali G, Narciso P, Notari S, Ascenzi P. The extraordinary ligand binding properties of human serum albumin. IUBMB life. 2005;57(12):787-96.

[68] Q. Li JH, B. Lu, H. Yao, WG Zhang, F. Ciprofloxacin-loaded bovine serum albumin microspheres: preparation and drug-release *in vitro*. Journal of Microencapsulation. 2001;18(6):825-9.

[69] Meziani MJ, Sun Y-P. Protein-conjugated nanoparticles from rapid expansion of supercritical fluid solution into aqueous solution. Journal of the American Chemical Society. 2003;125(26):8015-8.

[70] Lin W, Coombes AG, Garnett MC, Davies MC, Schacht E, Davis SS, Illum L. Preparation of sterically stabilized human serum albumin nanospheres using a novel Dextranox-MPEG crosslinking agent. Pharmaceutical Research. 1994;11(11):1588-92.

[71] Patil GV. Biopolymer albumin for diagnosis and in drug delivery. Drug Development Research. 2003;58(3):219-47.

[72] Jahanshahi M, Babaei Z. Protein nanoparticle: A unique system as drug delivery vehicles. African Journal of Biotechnology. 2008;7(25).

[73] Pinto Reis C, Neufeld RJ, Ribeiro AJ, Veiga F. Nanoencapsulation I. Methods for preparation of drug-loaded polymeric nanoparticles. Nanomedicine: Nanotechnology, Biology and Medicine. 2006;2(1):8-21.

[74] Bronich TK, Keifer PA, Shlyakhtenko LS, Kabanov AV. Polymer micelle with cross-linked ionic core. Journal of the American Chemical Society. 2005;127(23):8236-7.

[75] Yu S, Yao P, Jiang M, Zhang G. Nanogels prepared by self-assembly of oppositely charged globular proteins. Biopolymers. 2006;83(2):148-58.

[76] Qi J, Yao P, He F, Yu C, Huang C. Nanoparticles with dextran/chitosan shell and BSA/chitosan core—doxorubicin loading and delivery. International Journal of Pharmaceutics. 2010;393(1):177-85.

[77] Boye JI, Alli I, Ismail AA. Interactions involved in the gelation of bovine serum albumin. Journal of Agricultural and Food Chemistry. 1996;44(4):996-1004.

[78] Lee SH, Heng D, Ng WK, Chan H-K, Tan RB. Nano spray drying: a novel method for preparing protein nanoparticles for protein therapy. International Journal of Pharmaceutics. 2011;403(1):192-200.

[79] Pereverzeva E, Treschalin I, Bodyagin D, Maksimenko O, Langer K, Dreis S, Asmussen B, Kreuter J, Gelperina S. Influence of the formulation on the tolerance profile of nanoparticle-bound doxorubicin in healthy rats: focus on cardio-and testicular toxicity. International Journal of Pharmaceutics. 2007;337(1):346-56.

[80] Russell LD, Russell JA. Short-term Morphological response of the rat testis to administration of five chemotherapeutic agents. American Journal of Anatomy. 1991;192(2):142-68.

[81] Zucchi R, Danesi R. Cardiac toxicity of antineoplastic anthracyclines. Current Medicinal Chemistry-Anti-Cancer Agents. 2003;3(2):151-71.

[82] Singh HD, Wang G, Uludağ H, Unsworth LD. Poly-l-lysine-coated albumin nanoparticles: Stability, mechanism for increasing *in vitro* enzymatic resilience, and siRNA release characteristics. Acta Biomaterialia. 2010;6(11):4277-84.

[83] Zhang S, Wang G, Lin X, Chatzinikolaidou M, Jennissen HP, Laub M, Uludağ H. Polyethylenimine-coated albumin nanoparticles for BMP-2 delivery. Biotechnology Progress. 2008;24(4):945-56.

[84] Zhang S, Doschak MR, Uludağ H. Pharmacokinetics and bone formation by BMP-2 entrapped in polyethylenimine-coated albumin nanoparticles. Biomaterials. 2009;30(28):5143-55.

[85] Shen Z-Y, Ma G-H, Dobashi T, Maki Y, Su Z-G. Preparation and characterization of thermo-responsive albumin nanospheres. International Journal of Pharmaceutics. 2008;346(1):133-42.

[86] Shen Z, Wei W, Zhao Y, Ma G, Dobashi T, Maki Y, Su Z, Wan J. Thermosensitive polymer-conjugated albumin nanospheres as thermal targeting anti-cancer drug carrier. European Journal of Pharmaceutical Sciences. 2008;35(4):271-82.

[87] Kouchakzadeh H, Shojaosadati SA, Maghsoudi A, Farahani EV. Optimization of PEGylation conditions for BSA nanoparticles using response surface methodology. AAPS PharmSciTech. 2010;11(3):1206-

11.

[88] Lin W, Garnett MC, Davis SS, Schacht E, Ferruti P, Illum L. Preparation and characterisation of rose Bengal-loaded surface-modified albumin nanoparticles. Journal of Controlled Release. 2001;71(1):117-26.

[89] Rahimnejad M, Mokhtarian N, Ghasemi M. Production of protein nanoparticles for food and drug delivery system. African Journal of Biotechnology. 2009;8(19).

[90] Atkinson SF, Bettinger T, Seymour LW, Behr J-P, Ward CM. Conjugation of folate via gelonin carbohydrate residues retains ribosomal-inactivating properties of the toxin and permits targeting to folate receptor positive cells. Journal of Biological Chemistry. 2001;276(30):27930-5.

[91] Campbell IG, Jones TA, Foulkes WD, Trowsdale J. Folate-binding protein is a marker for ovarian cancer. Cancer Research. 1991;51(19):5329-38.

[92] Oyewumi MO, Mumper RJ. Influence of formulation parameters on gadolinium entrapment and tumor cell uptake using folate-coated nanoparticles. International Journal of Pharmaceutics. 2003;251(1):85-97.

[93] Liapis H, Adler LM, Wick MR, Rader JS. Expression of *αvβ3* integrin is less frequent in ovarian epithelial tumors of low malignant potential in contrast to ovarian carcinomas. Human Pathology. 1997;28(4):443-9.

[94] Bello L, Zhang J, Nikas DC, Strasser JF, Villani RM, Cheresh DA, Carroll RS, Black PM. *αvβ3* and *αvβ5* Integrin Expression in Meningiomas. Neurosurgery. 2000;47(5):1185-95.

[95] Kreuter J, Hekmatara T, Dreis S, Vogel T, Gelperina S, Langer K. Covalent attachment of apolipoprotein AI and apolipoprotein B-100 to albumin nanoparticles enables drug transport into the brain. Journal of Controlled Release. 2007;118(1):54-8.

[96] Zensi A, Begley D, Pontikis C, Legros C, Mihoreanu L, Wagner S, Büchel C, von Briesen H, Kreuter J. Albumin nanoparticles targeted with Apo E enter the CNS by transcytosis and are delivered to neurones. Journal of Controlled Release. 2009;137(1):78-86.

[97] Wartlick H, Michaelis K, Balthasar S, Strebhardt K, Kreuter J, Langer K. Highly specific HER2-mediated cellular uptake of antibody-modified nanoparticles in tumour cells. Journal of Drug Targeting.

2004;12(7):461-71.

[98] Wagner S, Rothweiler F, Anhorn MG, Sauer D, Riemann I, Weiss EC, Katsen-Globa A, Michaelis M, Cinatl Jr J, Schwartz D. Enhanced drug targeting by attachment of an anti αv integrin antibody to doxorubicin loaded human serum albumin nanoparticles. Biomaterials. 2010;31(8):2388-98.

[99] John TA, Vogel SM, Tiruppathi C, Malik AB, Minshall RD. Quantitative analysis of albumin uptake and transport in the rat microvessel endothelial monolayer. American Journal of Physiology-Lung Cellular and Molecular Physiology. 2003;284(1):L187-L96.

[100] Hawkins MJ, Soon-Shiong P, Desai N. Protein nanoparticles as drug carriers in clinical medicine. Advanced Drug Delivery Reviews. 2008;60(8):876-85.

[101] Minshall RD, Tiruppathi C, Vogel SM, Malik AB. Vesicle formation and trafficking in endothelial cells and regulation of endothelial barrier function. Histochemistry and Cell Biology. 2002;117(2):105-12.

[102] Vogel SM, Minshall RD, Pilipović M, Tiruppathi C, Malik AB. Albumin uptake and transcytosis in endothelial cells *in vivo* induced by albumin-binding protein. American Journal of Physiology-Lung Cellular and Molecular Physiology. 2001;281(6):L1512-L22.

[103] Cox B, Emili A. Tissue subcellular fractionation and protein extraction for use in mass-spectrometry-based proteomics. Nature Protocols. 2006;1(4):1872-8.

[104] Navarro A, Sánchez Del Pino MJ, Gómez C, Peralta JL, Boveris A. Behavioral dysfunction, brain oxidative stress, and impaired mitochondrial electron transfer in aging mice. American Journal of Physiology-Regulatory, Integrative and Comparative Physiology. 2002;282(4):R985-R92.

[105] Cossarizza A, Baccaranicontri M, Kalashnikova G, Franceschi C. A new method for the cytofluorometric analysis of mitochondrial membrane potential using the J-aggregate forming lipophilic cation 5, 5′, 6, 6′-tetrachloro-1, 1′, 3, 3′-tetraethylbenzimidazolcarbocyanine iodide (JC-1). Biochemical and Biophysical Research Communications. 1993;197(1):40-5.

[106] Singh R, Gregory C, Emery A. Cell death in bioreactors: a role for apoptosis. Biotechnology and Bioengineering. 1994;44(6):720-6.

[107] Brand K. Aerobic glycolysis by proliferating cells: protection against oxidative stress at the expense of energy yield. Journal of Bioenergetics and Biomembranes. 1997;29(4):355-64.

[108] Yang M, Butler M. Effects of ammonia on CHO cell growth, erythropoietin production, and glycosylation. Biotechnology and Bioengineering. 2000;68(4):370-80.

[109] Li J, Wong CL, Vijayasankaran N, Hudson T, Amanullah A. Feeding lactate for CHO cell culture processes: Impact on culture metabolism and performance. Biotechnology and Bioengineering. 2012;109(5):1173-86.

[110] Courtes FC, Vardy L, Wong NS, Bardor M, Yap MG, Lee D-Y. Understanding translational control mechanisms of the mTOR pathway in CHO cells by polysome profiling. New biotechnology. 2013).

[111] Dreesen IA, Fussenegger M. Ectopic expression of human *mTOR* increases viability, robustness, cell size, proliferation, and antibody production of chinese hamster ovary cells. Biotechnology and Bioengineering. 2011;108(4):853-66.

[112] Dorai H, Kyung YS, Ellis D, Kinney C, Lin C, Jan D, Moore G, Betenbaugh MJ. Expression of anti-apoptosis genes alters lactate metabolism of Chinese Hamster Ovary cells in culture. Biotechnology and Bioengineering. 2009;103(3):592-608.

[113] Majors BS, Betenbaugh MJ, Chiang GG. Links between metabolism and apoptosis in mammalian cells: applications for anti-apoptosis engineering. Metabolic Engineering. 2007;9(4):317-26.

[114] Plumb JA, Milroy R, Kaye S. Effects of the pH dependence of 3-(4, 5-dimethylthiazol-2-yl)-2, 5-diphenyltetrazolium bromide-formazan absorption on chemosensitivity determined by a novel tetrazolium-based assay. Cancer Research. 1989;49(16):4435-40.

[115] Cho K, Wang X, Nie S, Shin DM. Therapeutic nanoparticles for drug delivery in cancer. Clinical Cancer Research. 2008;14(5):1310-6.

[116] Gref R, Minamitake Y, Peracchia MT, Trubetskoy V, Torchilin V, Langer R. Biodegradable long-circulating polymeric nanospheres. Science. 1994;263(5153):1600-3.

[117] Wang AZ, Gu F, Zhang L, Chan JM, Radovic-Moreno A, Shaikh MR, Farokhzad OC. Biofunctionalized targeted nanoparticles for therapeutic applications. 2008).

[118] Kumar M. Nano and microparticles as controlled drug delivery devices. J Pharm Pharm Sci. 2000;3(2):234-58.

[119] Langer K, Balthasar S, Vogel V, Dinauer N, Von Briesen H, Schubert D. Optimization of the preparation process for human serum albumin (HSA) nanoparticles. International Journal of Pharmaceutics. 2003;257(1):169-80.

[120] Elzoghby AO, Samy WM, Elgindy NA. Albumin-based nanoparticles as potential controlled release drug delivery systems. Journal of Controlled Release. 2012;157(2):168-82.

[121] Ha S, Park T. Efficient production of recombinant protein in *Spodoptera frugiperda*/AcNPV system utilizing silkworm hemolymph. Biotechnology Letters. 1997;19(11):1087-91.

[122] Rhee WJ, Kim EJ, Park TH. Silkworm hemolymph as a potent inhibitor of apoptosis in Sf9 cells. Biochemical and Biophysical Research Communications. 2002;295(4):779-83.

[123] Kim EJ, Rhee WJ, Park TH. Inhibition of apoptosis by a *Bombyx mori* gene. Biotechnology Progress. 2004;20(1):324-9.

[124] Park JH, Lee JH, Park HH, Rhee WJ, Choi SS, Park TH. A protein delivery system using 30Kc19 cell-penetrating protein originating from silkworm. Biomaterials. 2012;33(35):9127–34.

[125] Von Storp B, Engel A, Boeker A, Ploeger M, Langer K. Albumin nanoparticles with predictable size by desolvation procedure. Journal of Microencapsulation. 2012;29(2):138-46.

[126] Langer K, Anhorn M, Steinhauser I, Dreis S, Celebi D, Schrickel N, Faust S, Vogel V. Human serum albumin (HSA) nanoparticles: reproducibility of preparation process and kinetics of enzymatic degradation. International Journal of Pharmaceutics. 2008;347(1):109-17.

[127] Scriver CR. The metabolic & molecular bases of inherited disease. 8th ed. New York: McGraw-Hill Professional; 2001, p. 3733–74.

[128] Lee K, Jin X, Zhang K, Copertino L, Andrews L, Baker-Malcolm J, Geagan L, Qiu H, Seiger K, Barngrover D. A biochemical and pharmacological comparison of enzyme replacement therapies for the glycolipid storage disorder Fabry disease. Glycobiology. 2003;13(4):305-13.

[129] Linthorst GE, Hollak CE, Donker-Koopman WE, Strijland A, Aerts JM.

Enzyme therapy for Fabry disease: neutralizing antibodies toward agalsidase alpha and beta. Kidney International. 2004;66(4):1589-95.

[130] Vedder AC, Linthorst GE, Houge G, Groener JE, Ormel EE, Bouma BJ, Aerts JM, Hirth A, Hollak CE. Treatment of Fabry disease: outcome of a comparative trial with agalsidase alfa or beta at a dose of 0.2 mg/kg. PloS One. 2007;2(7):e598.

[131] Ha SH, Park TH, Kim S-E. Silkworm hemolymph as a substitute for fetal bovine serum in insect cell culture. Biotechnology Techniques. 1996;10(6):401-6.

[132] Lee HJ, Park HH, Kim JA, Park JH, Ryu J, Choi J, Lee J, Rhee WJ, Park TH. Enzyme delivery using the 30Kc19 protein and human serum albumin nanoparticles. Biomaterials. 2014;35(5):1696-704.

[133] Yamada Y, Akita H, Kogure K, Kamiya H, Harashima H. Mitochondrial drug delivery and mitochondrial disease therapy–an approach to liposome-based delivery targeted to mitochondria. Mitochondrion. 2007;7(1):63-71.

[134] Goswami J, Sinskey A, Steller H, Stephanopoulos G, Wang D. Apoptosis in batch cultures of Chinese hamster ovary cells. Biotechnology and Bioengineering. 1999;62(6):632-40.

[135] Arden N, Betenbaugh MJ. Life and death in mammalian cell culture: strategies for apoptosis inhibition. Trends in Biotechnology. 2004;22(4):174-80.

[136] Lao MS, Toth D. Effects of ammonium and lactate on growth and metabolism of a recombinant Chinese hamster ovary cell culture. Biotechnology Progress. 1997;13(5):688-91.

[137] Zagari F, Jordan M, Stettler M, Broly H, Wurm FM. Lactate metabolism shift in CHO cell culture: the role of mitochondrial oxidative activity. New biotechnology. 2013;30(2):238-45.

[138] Harush-Frenkel O, Rozentur E, Benita S, Altschuler Y. Surface charge of nanoparticles determines their endocytic and transcytotic pathway in polarized MDCK cells. Biomacromolecules. 2008;9(2):435-43.

[139] Schnitzer J. gp60 is an albumin-binding glycoprotein expressed by continuous endothelium involved in albumin transcytosis. American Journal of Physiology. 1992;262(1 Pt 2):H246-54.

[140] Rybin VO, Xu X, Lisanti MP, Steinberg SF. Differential Targeting of β-Adrenergic Receptor Subtypes and Adenylyl Cyclase to Cardiomyocyte

Caveolae; a Mechanism to Functionally Regulate the cAMP Signaling Pathway. Journal of Biological Chemistry. 2000;275(52):41447-57.

[141] Wang L, Connelly MA, Ostermeyer AG, Chen H-h, Williams DL, Brown DA. Caveolin-1 does not affect SR-BI-mediated cholesterol efflux or selective uptake of cholesteryl ester in two cell lines. Journal of Lipid Research. 2003;44(4):807-15.

[142] Yang J-P, Ma X-X, He Y-X, Li W-F, Kang Y, Bao R, Chen Y, Zhou C-Z. Crystal structure of the 30K protein from the silkworm *Bombyx mori* reveals a new member of the β-trefoil superfamily. Journal of Structural Biology. 2011;175(1):97-103.

[143] Park HH, Sohn Y, Yeo JW, Park JH, Lee HJ, Ryu J, Rhee WJ, Park TH. Identification and characterization of a novel cell-penetrating peptide of 30Kc19 protein derived from *Bombyx mori*. Process Biochemistry. 2014;49(9):1516-26.

# 국 문 초 록

## 약물 전달에 응용하기 위한 30Kc19를 이용한 단백질 나노입자의 제조 및 특성 연구

이 홍 재
서울대학교 대학원
화학생물공학부

30kc19 단백질은 30 kDa의 분자량을 갖는, 누에에서 유래한 30K 단백질 족의 하나이다. 30Kc19 단백질은 누에 체액 내 30K 단백질 중 가장 많은 양을 차지한다. 이전의 연구에서, 유전자 발현 혹은 대장균에서 생산한 재조합 단백질 형태의 30K 단백질들이 항에이파토시스 효과를 보이는 것이 보고되었으며 30Kc19 단백질의 경우 유전자 발현 혹은 재조합 단백질 형태로 재조합 단백질의 생산성과 당쇄화를 촉진하는 효과를 얻은 바 있다. 뿐만 아니라, 30Kc19 단백질은 생체 외에서 효소 활성화와 세포 통과 효과를 보였다.

이 연구에서는 30Kc19 단백질이 세포 내로 투과하여 세포 내 효소를 안정화시킨다는 가설을 세우고, 이를 생체 외와 세포 실험을 통하여 확인하였다. 세포에서 분리한 미토콘드리아 효소 복합체 I / III의 활성은 30Kc19의 투여

량에 비례하여 증가하였으나 초기 반응속도에는 영향을 주지 않았으며, 이는 30Kc19가 효소의 비활성 보다는 세포 안정성을 증대시켰음을 암시한다. 세포 내 효소 활성 실험에서, HeLa 세포 내 미토콘드리아 효소 복합체 II의 활성이 30Kc19에 의하여 50% 이상 증대됨을 관찰하였다. 또한, 증대된 HeLa 세포 내 미토콘드리아 효소 복합체 활성은 미토콘드리아의 막전위와 ATP 생산량을 50% 이상 증대시키는 것을 관찰할 수 있었다.

다음으로, 30Kc19 단백질의 세포 투과성과 효소 안정화 효과가 약물 전달에 활용되었다. 30Kc19 단백질의 효과와 함께 인간혈청알부민(HSA) 나노입자의 안정성을 동시에 얻기 위하여, 두 단백질이 나노입자를 만드는 재료로 활용되었다. 30Kc19-HSA 나노입자는 탈용매화 방법에 의해 성공적으로 합성되었으며, 균일한 구형의 형태와 안정적인 분산을 보였다. 30Kc19-HSA 나노입자는 세포에 처리하였을 때 거의 독성을 보이지 않았으며, HSA 나노입자에 비해 증가된 세포 도입량을 보였다.

안정적인 형태의 30Kc19-HSA 나노입자가 성공적으로 합성되었기 때문에, 30Kc19 단백질이 단백질 화물에 미치는 영향을 알아보기 위하여 모델 효소가 나노입자에 충진되었다. 베타갈락토시데이즈가 충진된 30Kc19-HSA 나노입자는 균일한 구형으로 합성되어 PBS와 세포배양배지 내에서 일정하게 분산되었으며, 충진된 베타갈락토시데이즈는 서방형 방출 양상을 보였다. 베타갈락토시데이즈가 충진된 30Kc19-HSA 나노입자는 세포 내에서 거의 독성을 보이지 않았으며, HeLa 세포와 HEK293 세포를 이용한 실험에서 HSA 나노입자에 비해 향상된 세포 도입량과 세포 내 베타갈락토시데이즈 활성을 나타냈다.

다음으로, 30Kc19-HSA 나노입자는 실제 치료용 단백질을 세포에 전달하

는 데 사용되었다. 패브리병은 알파갈락토시데이즈의 결핍으로 인해 리소좀으로 운반된 자연적인 글리코스핑고리피드를 분해하지 못하여 발생하는 리소조말 축적 유전질환이다. 재조합 알파갈락토시데이즈를 이용한 효소보충요법(ERT)이 패브리병의 유일한 치료법이나, 효율적인 치료를 위해서 알파갈락토시데이즈를 세포 내에 효율적으로 운반하고 세포 내 활성을 유지시키는 것이 문제가 되고 있다. 따라서, 30Kc19-HSA 나노입자가 효율적인 알파갈락토시데이즈의 세포 도입과 안정성을 증대시키기 위하여 사용되었다. 알파갈락토시데이즈가 충진된 30Kc19-HSA 나노입자 역시 균일한 구형으로 합성되었고, 세포배양배지 내에 고르게 분산되었다. 30Kc19-HSA 나노입자는 인간피부세포에 처리하였을 때 독성이 거의 없었으며, 증가된 세포 도입량과 세포 내 알파갈락토시데이즈 활성 유지를 보였다. 뿐만 아니라, 실제 패브리병 환자의 인간피부세포를 이용한 실험에서, 30Kc19-HSA 나노입자는 증가된 글로보트리아오실세라마이드(Gb3) 분해 능력을 보였다. 이상의 실험에서, 30Kc19-HSA 나노입자는 단백질 치료제의 효율적인 세포 전달과 안정성 향상을 위한 효율적인 도구로 쓰일 수 있을 것으로 기대되었다.

주요어: 30Kc19 단백질, 미토콘드리아 효소 복합체, 효소 안정성, 단백질 나노입자, 약물 전달, 패브리병

**학번**: 2006-21377